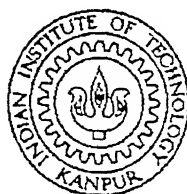


# COHERENT AND SQUEEZED ANGULAR MOMENTUM STATES IN SCHWINGER REPRESENTATION WITH APPLICATIONS TO QUANTUM OPTICS

*A Thesis Submitted*  
in Partial Fulfillment of the Requirements  
for the Degree of  
Doctor of Philosophy

*by*  
ABIR BANDYOPADHYAY



*to the*  
DEPARTMENT OF PHYSICS  
INDIAN INSTITUTE OF TECHNOLOGY, KANPUR  
December, 1996

13 JUL 1988

LIBRARY  
I.I.T., KANPUR

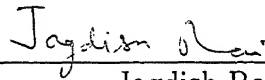
**A 125703**

PHY-1996-D-BAN-COH



# CERTIFICATE

It is certified that the work contained in this thesis entitled *Coherent and Squeezed angular momentum states in Schwinger representation with applications to quantum optics* by *Abir Bandyopadhyay* has been carried out under my supervision and that this work has not been submitted elsewhere for a degree.



---

Jagdish Rai  
Department of Physics  
Indian Institute of Technology  
Kanpur

December, 1996





# Acknowledgments

It is my pleasure to thank Dr. Jagdish Rai for introducing me to the subject of quantum optics and supervising my thesis, after the terminal illness of my previous supervisor, late Prof. S. K Sharma, who taught me the beauties of angular momentum systems. I thank Dr. V. Ravishankar for evaluating me at every stage of my doctoral programme and Dr. S. Saha and Dr. M. K. Verma for being present in my peer group review committees. I specially acknowledge the moral support rendered by Prof. A. K. Majumder, then Head of the Department, at the time of Late Prof. Sharma's illness. I would also like to acknowledge Dr. Sayan Kar for his help in deciding my field of work and Mr. S. Anantha Ramakrishna for a collaborative work which is included in this thesis. I thank the faculties and friends from different institutions with whom I have shared many intriguing discussions regarding the work presented in this thesis.

It is futile to name the acquaintances I have enjoyed in this campus and surroundings, especially at hall IV, Physics department, and our drama group. Special mention has to be made about Mr. G. K. Singh for his  $\text{\LaTeX}$  expertise. I would like to thank them collectively. I will not be able to forget my notorious batchmates in the department. Finally I acknowledge my parents whose silent support can not be repaid.

Abir Bandyopadhyay

# List of published/submitted papers

- Journal:

1. 'Uncertainties of Schwinger angular-momentum operators for squeezed radiation in interferometers' by **Abir Bandyopadhyay** and Jagdish Rai, Phys. Rev. A **51**, 1597 (1995).
2. 'A dissipative quantum mechanical beam-splitter' by S. Anantha Ramakrishna, **Abir Bandyopadhyay**, and Jagdish Rai, (communicated).
3. 'Transfer of non-classical properties through dual channel directional coupler' by **Abir Bandyopadhyay** and Jagdish Rai, (communicated).
4. 'Schwinger angular momentum coherent state representation for two Bose-Einstein condensates and their interaction with a resonant coherent radiation' by **Abir Bandyopadhyay** and Jagdish Rai, (communicated).
5. 'Geometrical representation of angular momentum coherence and squeezing' by Abir Bandyopadhyay and Jagdish Rai, (communicated).
6. 'Angular constraints in cold d-t fusion catalyzed by negative muons' by Lali Chatterjee and **Abir Bandyopadhyay**, Ind. J. Phys. **64 A**, 160 (1990)\*.
7. 'Squeezing in molecular anharmonic excitations' by Arnab Majumdar, Kingshuk Ghosh, **Abir Bandyopadhyay**, Jagdish Rai, and M. K. Verma (communicated)\*.

• **Conference/Workshop Proceedings :**

1. 'Optical interferometry with squeezed radiation' by **Abir Bandyopadhyay** and Jagdish Rai, *Proceedings of Workshop On Advanced Laser Spectroscopy 1995 (WOALS'95)*, ed. H. D. Bisht, R. K. Thareja, A. Pradhan and P. K. Khulbe, Allied Publishers, 257 (1995).
2. 'Quantum mechanical reflection with losses' by S. Anantha Ramakrishna, **Abir Bandyopadhyay** and Jagdish Rai, *Proceedings of WOALS'95*, 255 (1995).
3. 'Squeezing and amplification without inversion in the interaction of coherent radiation and two level atoms' by **Abir Bandyopadhyay** and Jagdish Rai, *Proceedings of International Symposium on Atomic Coherence and Inversionless Amplification 1995*, ed. J. Y. Gao and S.-Y. Zhu, 104 (1996).
4. 'Transfer of non-classical properties in an optical dual-channel coupler' by **Abir Bandyopadhyay** and Jagdish Rai, *Proceedings of Conference on Laser and Electron Optics/ Quantum Electronics and Laser Sciences*, (1996).
5. 'Squeezing in molecular vibrational excitations' by Arnab Majumdar, Kingshuk Ghosh, **Abir Bandyopadhyay**, Jagdish Rai, and M. K. Verma (accepted in *International conference on quantum optics and laser physics (IC-QOLP)*, to be held in Jan. 3-6, 1997, at Hong Kong Baptist University)\*.

\*Work not related to this thesis.

# Synopsis

Coherent and squeezed states of radiation are of great current interest. These states have many potential application in technology and in understanding the basic laws of nature. Several attempts have been made in the past to study the coherent states of angular momentum (AM) systems [1,2]. Few questions arise in the definitions AM coherent states in terms of squeezing. Squeezed AM states are yet to be defined properly. In the present thesis I study the coherent AM states and define squeezed AM states using Schwinger representation of AM [3]. I apply coherent AM states to two (optical and atomic) physical systems. The squeezed AM states are shown to have application in interferometry and in control of squeezing. The interaction of a resonant radiation with coherent two level atomic system promises to generate squeezed angular momentum states in the atomic system.

The first chapter introduces the subject with the motivation of the present thesis. The second chapter presents the basic definitions of coherent and squeezed states of harmonic oscillator with few of their important properties. The particles in the oscillator potential are assumed to follow Bose Einstein statistics. It also associates coherent states of harmonic oscillator to two of the physical systems corresponding to light (Laser) and atoms (ultracold ensemble). Though the former is responsible for most of the developments of the coherent states, recent technological breakthrough has been able to create samples of atoms with thermal de Broglie wavelength as large as its macroscopic sample size, which is fulfilled at very low temperature and high densities. At such low temperatures ( $10^{-8} - 10^{-6}$  Kelvin) and high densities ( $10^{10} - 10^{14} \text{ cm}^{-3}$ ) the atoms loose their individual identity and behave as a single

macroscopic quantum state similar to the role of lasers in conventional coherent optics. The association of squeezed states to physical systems presented in this chapter are in context to light only.

The third chapter introduces the two definitions of coherent states of AM due to Atkins [1] (we call these as Schwinger AM coherent or SAMC states) and Arecchi [2] (generally referred as atomic coherent states). Both the definitions are compared in terms of classical or quantum nature of the physical system. A geometrical representation in the AM space allows better understanding of the nature of the phase space distribution. By performing squeezing transformation on the bosonic coherent states generalize the idea of SAMC states to Schwinger Angular Momentum Squeezed (SAMS) states. I show that SAMS states, constructed from the bosonic squeezed coherent states, exhibit squeezing of AM operators under certain range of parameters. The properties of these states were studied and compared with their single mode bosonic counterpart. I show the nature of the phase space distribution of the SAMS states via the geometrical representation by plotting the uncertainty ellipsoid in the AM space. I also discuss the discrepancies in the definition of squeezing in AM space and how SAMC states overcome this over the atomic coherent states giving rise to the SAMS states a different status of squeezing.

The fourth chapter deals with the applications of SAMC and SAMS states in context of two mode radiation. Three applications are considered, one for the SAMC state and two for the SAMS state. The SAMC states are used to analyze a dissipative beam-splitter (BS), by modeling the losses in the BS due to the excitation of optical phonons. The action of the BS results in a rotation in AM space. The losses are obtained in terms of the BS medium properties. Using second order perturbation the model yields Beer's law for absorption in the first approximation. It is shown that the fluctuations in the modes get increased because of the losses. The results show the existence of quantum interference due to phase correlations between the input beams. Hence in spite of having such a dissipative medium, it is possible to design a lossless 50-50 BS at normal incidence which have potential applications in

dielectric-coated mirrors.

In the same chapter SAMS states were applied to increase the accuracy of interferometers and coupling of two radiations via directional coupler. It is shown that arbitrary increase in squeezing does not increase the accuracy of a Mach-Zehnder interferometer. The estimate of the value of the amount of squeezing for the most accurate interferometric measurement is given. It is also noted that double mode squeezing deteriorates the accuracy of the interferometer in comparison to single mode squeezing. The coupling in the dual channel directional coupler, treated as coupled harmonic oscillator (CHO), is represented by a continuous rotation in the AM space. The motivation of the application is to control quantum properties of one light beam by another. Under the rotating wave approximation (RWA), it is shown that, if initially one of the modes is coherent and the other one squeezed, then the squeezing and non-Poissonianness of the photon statistics can be transferred from one mode to the other. It is also shown that the transferred squeezing to the initially coherent mode is of new type. In the affected mode the squeezed quadrature remains squeezed, whereas the other quadrature is antisqueezed throughout except at the points where both of them return to coherent value. A parametric study of these properties, depending upon interaction time and the degree of initial squeezing in one of the modes, is presented.

In the fifth chapter the SAMC states are applied to atomic system. By exploiting the property that the ultracold atoms are represented by coherent states, I express an ultracold ensemble of atoms in its ground state and one of its excited states near the ground one as SAMC states. The AM vector represents the Bloch vector of the atomic system. The Jaynes-Cummings interaction of a coherent radiation with an ensemble of ultracold bosonic two level atoms, represented by SAMC states, is studied under RWA. The frequency of the coherent radiation is resonant with the spacing between the levels. The results show generation of squeezing and other nonclassical properties like photon antibunching of radiation, and amplification without population inversion. The interaction also decreases the uncertainties of the AM i quadratures

promising possibility of generation of squeezed angular momentum states in atomic system.

Finally the chapter six concludes the work presented in the thesis emphasizing the main aspects. It also deals in short about other applications, not considered in the thesis.

#### **References :**

1. P. W. Atkins and J. C. Dobson, Proc. R. Soc. London, Ser. A **321**, 321 (1971).
2. F. T. Arecchi, E. Courtens, R. Gilmore and H. Thomas, Phys. Rev. A **6**, 2211 (1972).
3. J. Schwinger, in *Quantum theory of angular momentum*, ed. L. Beidenharn and H. van Dam, Academic press, NY, 229 (1965).

# Contents

Acknowledgments	iii
List of published/communicated papers	iv
Synopsis	vi
List of Figures	xiv
<b>1 Introduction</b>	<b>1</b>
<b>2 Coherent and squeezed states of harmonic oscillator</b>	<b>10</b>
2.1 Coherent states . . . . .	10
2.1.1 Definitions of coherent states . . . . .	11
2.1.2 Properties of coherent states . . . . .	12
2.1.3 Number statistics . . . . .	14
2.1.4 Physical systems represented by coherent states . . . . .	14
2.2 Squeezed states . . . . .	15
2.2.1 Definitions of squeezed states . . . . .	16
2.2.2 Phase space diagram . . . . .	17
2.2.3 Number distribution . . . . .	18
<b>3 Coherent and squeezed angular momentum states</b>	<b>19</b>
3.1 Uncertainty relations of angular momentum . . . . .	21
3.2 Angular momentum coherent states . . . . .	21



3.2.1	Coherent spin states . . . . .	22
3.2.2	Angular momentum coherent states in Schwinger representation	27
3.3	Angular Momentum Squeezed States . . . . .	31
3.3.1	Single mode squeezing . . . . .	32
3.3.2	Double mode squeezing . . . . .	37
4	<b>Applications to two mode radiation system</b>	40
4.1	Lossy BS . . . . .	41
4.1.1	Representation of a BS in AM space . . . . .	43
4.1.2	Radiation field-phonon interaction . . . . .	45
4.1.3	Lossy medium . . . . .	50
4.1.4	Lossy Beam-Splitter . . . . .	51
4.2	Transfer of nonclassical properties in dual channel directional coupler	53
4.2.1	Dual channel coupler as a time dependent continuous rotator	55
4.2.2	Time evolution of the operators . . . . .	55
4.2.3	Transfer of squeezing . . . . .	56
4.2.4	Transfer of nonclassical number statistics . . . . .	58
4.3	Application to Interferometry . . . . .	60
4.3.1	Mach-Zender interferometer . . . . .	60
4.3.2	Previous developments . . . . .	61
4.3.3	Present results . . . . .	61
5	<b>Application in two level atomic system</b>	64
5.1	Hamiltonian of the interaction . . . . .	64
5.2	Time development of the operators . . . . .	65
5.3	Initial state of the combined system . . . . .	66
5.4	Evolution of the field observables . . . . .	66
5.5	Evolution of the atomic observables . . . . .	68
6	<b>Conclusion</b>	70

Appendix	75
Bibliography	79

# List of Figures

2.1	Phase space diagram of coherent and vacuum states of a harmonic oscillator. . . . .	14
2.2	Phase space diagram of squeezed states of a harmonic oscillator. . . .	17
3.1	The rotation caused by the rotation operator defined in equation 3.6 .	23
3.2	The rotation of CSS generates SSS. Notice the projection of the CSS on X-Y plane. . . . .	26
3.3	The phase space diagrams for SAMC states in two directions are shown. The projection of the uncertainty sphere on X-Y plane is always circular. . . . .	30
3.4	Parametric dependences of the quadratures. (a) Variation of $\mathcal{A}_+$ , $\mathcal{A}_-$ and their product <i>w.r.t.</i> $r$ for $j = 50$ , $m = -50$ and $\delta = 0$ . (b) Variation of $\mathcal{A}_-$ with $r$ for different $\delta$ with $j = 50$ , $m = -50$ . (c) Variation of $\mathcal{A}_-$ with $r$ for $j = 50$ , $\delta=0$ and $m = -50, -30, -10$ . (d) Variation of $\mathcal{A}_-$ with $r$ for $m = -20$ , $\delta = 0$ and $j = 20, 40, 60$ . . . . .	34
3.5	Schematic phase space diagram of SAMS state at pole. . . . .	36
3.6	Comparison between single mode and double mode squeezing. (a) Variation of $J_x$ , $J_y$ and their product with $r$ for single mode squeezing with $j = 50$ , $\delta=0$ and $m = -50$ , (b)Variation of $J_x$ , $J_y$ and their product with $r$ for double mode squeezing with $j = 50$ , $m = -50$ , $\theta=0$ and $r_{\pm} = r$ . . . . .	38
4.1	A beam-splitter with input and output light beams . . . . .	43

4.2	Lattice displacements due to optical phonons : (a) transverse, (b) longitudinal. . . . .	46
4.3	Dual Channel coupler with coupling controlled by Pockel's effect . .	54
4.4	Variations of the quadrature uncertainties of both the modes with time for different $r$ : (a) and (b) are the first and second quadratures of the first mode; (c) and (d) are the first and second quadratures of the second mode. . . . .	57
4.5	Variation of the statistical parameters of the (a) first mode and (b) second mode with time for different $r$ . . . . .	59
4.6	A typical Mach-Zehnder interferometer with two ports and a phase shifter. . . . .	60
4.7	Variation of $\Delta\Phi$ with $r$ for $n_+ = n_- = 16.0$ and $\theta_+ = \theta_- = \frac{\pi}{2}$ . . . . .	62
5.1	Variation of the uncertainties of the field quadratures with time . . .	67
5.2	Variation of the uncertainties of the normalized atomic quadratures with time. . . . .	69

# Chapter 1

## Introduction

Since the advent of the lasers in the early sixties, the study of coherent states has become a subject of great interest. The theoretical[1–3], as well as experimental developments in the field of quantum optics[4] have revived the interest in construction of classical states of quantum signature or *coherent states*. As early as 1926, Schrödinger conceived the idea of coherent states as minimum uncertainty wave packets[5]. For the last three decades, the development in the field of coherent states of several physical systems has been proven to be worth studying due to several interesting applications. A good collection of articles is available in reference[6], which deals in detail the mathematical developments of the notion of so called coherent states, suitable for different physical applications.

The coherent states of the harmonic oscillator are obtained by <sup>applying</sup> ~~operating~~ the displacement operator[2, 3, 6, 7] on the vacuum or ground state. These states have the same Gaussian dependence on space or momentum coordinates as of ground state of a harmonic oscillator, with the mean displaced by a constant amount from zero, the value for the ground state. The harmonic oscillator phase space description of electromagnetic fields has had great success in understanding the semiclassical and quantum theories of coherent light[6]. Coherent states are also defined as minimum uncertainty states, with equal value of the variances of the quadratures in the phase space. The product of the uncertainties in the quadratures is minimum

for these states and both the quadratures have equal uncertainties  $\frac{1}{\sqrt{2}}$ . In the first section of the next chapter, I present the definitions of coherent states of harmonic oscillator along with some basic properties.

In the same section I also introduce the atomic and radiation systems described by coherent states. The coherent radiation system was the first studied and experimentally produced. A similar atomic system can be achieved if the de Broglie wave length of a single atom is comparable to the sample size. During the last decade rapid progress has been made in the area of cooling and trapping of atoms. By combination of different cooling and trapping techniques the atoms could be kept at very low temperature (1-100  $\mu\text{K}$ ) and high density ( $10^{10} - 10^{13} \text{ cm}^{-3}$ )[8]. More recently, further developed techniques has been reported to achieve *Bose Einstein condensate* (BEC) at densities  $10^{12} - 10^{14} \text{ cm}^{-3}$  and temperatures  $10^{-8} - 10^{-7}$  Kelvin[9–11]. At such temperatures and densities the samples reach the critical points of BEC and the effect of quantum statistics becomes crucially important[12]. However, such atomic systems are expected to have properties similar to the <sup>332</sup>role of lasers in conventional coherent optics[13]. This property allows one to express a condensate by simplistic representation of coherent state of a harmonic oscillator.

During the last decade, considerable amount of work has been done in understanding and generating nonclassical states of radiation. While the coherent states of radiation are quantum states showing near classical properties with only the minimum amount of quantum noise (standard quantum limit or SQL) in both of the quadratures, the squeezed states are purely non-classical with noise in one quadrature reduced below the SQL at the expense of the other. Squeezed states show other non-classical properties as non-Poissonian photon statistics and antibunching. These states are useful to experiments answering several questions about the foundation of quantum mechanics[14]. Yuen[15] defined the em general coherent states, which can be experimentally produced using optical conjugation[16]. Similar non-classical states of radiation have been experimentally produced by nonlinear interactions of coherent radiation with matter, namely  $\chi^{(2)}$  and  $\chi^{(3)}$ , of radiation with matter and

extensively studied[14, 17]. The former process in the matter-radiation interaction, being of much stronger than the later one is a popular source to achieve squeezing. The action of the squeezing operator[18, 19], describing the former process, on the coherent state or vacuum produces the squeezed state.

The geometrical description of the Heisenberg uncertainty relation of two non-commuting variables (quadratures) is well known to give a better understanding of the inherent fluctuation due to the quantum nature of the squeezed light. Squeezing redistributes the uncertainties of the two quadratures resulting in one of them having less than its value for the coherent state at the expense of increasing the other[14, 18]. Due to the action of the squeezing operator the minimum uncertainty circle of the coherent or vacuum states in the phase space is squeezed to an ellipse. The lengths of the axes of the ellipse are related to the radius of the circle through squeezing parameter. The quadratures of the phase space retain the minimum uncertainty nature of vacuum or the coherent states. Quantitatively, the area of the minimum uncertainty circle for the coherent or ground state is same as the squeezed ellipse and the uncertainty product is  $\frac{1}{2}$ . It is by now well established that these states have many potential applications in improving the sensitivity of interferometers[20–22] and in noise-free transmission of information[23]. The last section of chapter 2 introduces the notion, along with other nonclassical properties, of squeezed states of harmonic oscillator.

The angular momentum (AM) is successful in describing the two mode radiation system or an ensemble of two-level bosonic particles besides the physical systems having intrinsic spin or orbital AM. Two radiation modes and two energy level systems are of special interest in the research of quantum optics due to simplicity and wide range of applications. The pseudo angular momentum vector is the Bloch vector or the dipole vector for the two level system[24]. The total angular momentum is a measure of the total number of particles in the modes of radiation or levels of the two level system. The AM projection represents the population difference between the modes or levels. The first section of the chapter 3 introduces the commutation

relations followed by the AM and phase operators.

Considerable amount of work has also been done in order to understand the coherent spin or angular momentum (AM) states[25–28]. There are two definitions of AM coherent states. In the next section I present the two definitions of coherent states with their properties. The first definition, discussed in the first subsection, is due to two simultaneous work of Radcliffe and Arecchi et al[25, 26]. I have referred these states as *coherent spin states* (CSS). I present the physical systems they represent in terms of two mode radiation and two level atoms. While these states are extensively used to describe atomic systems of classical nature, represented by number states, they can not describe the same for radiation systems. The reason is that there can be atomic systems of fixed number, but till date number state of radiation could not be produced despite several proposals. From the definition of squeezing and CSS a question has been raised[29–31] if they qualify as *squeezed spin states*. Arvind[32] has shown that the generators of  $U(2)$ , subgroup of  $Sp(4, \mathbb{R})$ , describing two mode system of quadratic operators, does not affect the degree of squeezing. Thus rotation, a generator of  $SU(2)$  group, which is a subgroup of  $U(2)$ , can not change introduce further squeezing. It is also noted that rotation does not change the state of the system. It is discussed geometrically how CSS can show squeezing in specific coordinate system.

Schwinger[33] developed a bosonic representation of the angular momentum (AM) where two sets (up and down) of bosonic creation (annihilation) operators create (annihilate) a  $\frac{1}{2}$  spin in that direction. The AM operators were expressed completely by the bosonic operators connecting both representations. He also studied the rotation and coupling of two or more AM vectors in this representation. Atkins and Dobson[28] constructed coherent AM states using the Schwinger bosonic representation and operating the displacement (coherent) operator on both of the bosonic vacuum states. These states were successfully applied by Fonda et.al to nuclear and molecular coherent rotational states[34]. I refer these states as em Schwinger angular momentum coherent (SAMC) states. SAMC states represent two types of physical



systems : a) a two mode coherent radiation system and b) ultracold ensemble of bosonic atoms in its ground and one of the excited states. While the first application is widely used, the second one was mentioned only by Fonda et al. in the context of coherent rotational states of nuclei and molecules. An ensemble of ultra-cold atoms in its ground state and another excited state can be represented by the SAMC states, as the atoms at each state behaves like a single mode laser. After the experimental achievement of BEC, application of such states to matter interferometry[35] is being investigated. In this subsection I introduce the SAMC state with the physical systems they represent. SAMC states were geometrically compared with the CSS to qualify as a better candidate for the definition of coherent states of AM.

Recently, the authors in Ref.[29] have discussed about the production and applications of squeezed spin states. They have proposed two types of interaction involving quadratic AM operators to correlate the individual spins and generate squeezing. In the last section of chapter 3 I generalize the idea of SAMC states to em Schwinger angular momentum squeezed (SAMS) states by performing squeezing transformation on the bosonic coherent states. I show that SAMS states, constructed from the bosonic squeezed coherent states, exhibit squeezing of Schwinger angular momentum operators under certain range of parameters. The properties of these states were studied and compared with their single mode bosonic counterpart. The nature of the phase space distribution for the SAMS states is shown geometrically in the AM space. The squeezing properties of SAMS and SAMC states does not pose any threat to the definition of squeezing in AM space.

In the fourth chapter I apply the different states, discussed in the previous one, to two mode radiation system such as interferometers. Beam splitter (BS) is an indispensable part of interferometers. Several authors have considered the behavior of the lossless quantum mechanical beam-splitter[36, 37]. Unlike the classical case where merely the energy in one beam is split into two parts, a quantum-mechanical analysis shows that the BS modifies the basic statistical properties of the beams[37, 38]. Thus a simple BS can be used to probe the quantum nature of light by simple yet

subtle experiments[39]. A BS offers one of the simplest interaction of a light mode with an external environment. It has been shown that damping of a mode due to interaction with a dissipative Gaussian reservoir can be approximated by a heuristic beam-splitter model[40]. The BS action can be described by a scattering represented by a rotation in the AM space[20, 37]. In the first section of this chapter, I present a model for lossy BS, where the losses are assumed to be due to optical phonons.

In the first subsection of this section, I review the lossless BS. Next subsection develops a model of losses in a medium due to the excitation of optical phonons in the medium. The lattice vibrations are accurately described by a harmonic oscillator model. The radiation is coupled to the phonon system. Thus the light-matter interaction is modeled in a simple manner and thus instructive. Most models of the interactions use advanced mathematical techniques. We have attempted to give a physical picture while keeping the mathematics as simple as possible. The model is true to a large extent in a host of dielectric materials in the microwave and the infra-red regions. It uses a second order perturbation and yields Beer's law for absorption in the first approximation. The BS is modeled as a reservoir of phonons at some finite temperature. We further assume that the photon-phonon interaction does not disturb the thermal equilibrium of the phonon system. Then the model is applied to a lossy BS to see its effects on the light modes. The losses are obtained in terms of the BS medium properties. It is shown that the fluctuations in the modes get increased because of the losses. The existence of quantum interferences due to phase correlations between the input beams is shown. It is found that in spite of having such a dissipative medium, it is possible to design a lossless 50-50 BS at normal incidence which may have potential applications in dielectric-coated mirrors.

An important goal for the future is the development of all-optical control logic systems in which one light beam is controlled by another light. These optically controlled logic systems have wide application in optical communication and in the concept of quantum computers. Optical communications involve operations like propagation, modulation, switching and frequency selection of radiation fields.

With the advent of squeezed radiation[14, 18] it has now become possible to operate the devices at lower noise levels i.e. with higher precisions. In the frame work of quantum optics devices employing control of light by another light could be well described by a simple model of two coupled harmonic oscillators[4]. There have been several attempts to study this kind of coupled harmonic oscillator interactions. A classical analysis of two coupled modes show that the two coupled modes exchange energies while propagating[41]. Love et al. studied the exchange of energy in beam propagation through a dual channel directional coupler[42]. When radiation passes through the coupler, exchange of power between the channels is possible because of the evanescent field present in the region between them. Lai et al. have discussed the photon statistics of non-classical fields in a linear directional coupler, where the losses can be negligible, using the number state as one of the inputs[43].

The question naturally arises is that how do the non-classical properties are exchanged in the coupled harmonic oscillators during propagation. Will it be possible to transfer the non-classical properties like squeezing and photon antibunching from one mode to the other? This could have far reaching applications in experimental field where two modes could be chosen to be widely different in frequencies. If it is possible to transfer squeezing then in principle one could apply the scheme to generate squeezed light at higher frequencies where it may not be feasible otherwise. In the next section of chapter four, I analyze the quantum uncertainties and the photon statistics in the interaction between the two modes of radiation, represented by a continuous rotation in the AM space, by treating as coupled harmonic oscillator (CHO) with the motivation of controlling quantum properties of one light beam by another. The interaction of CHO can also be applied to study thick BS, modeled with or without losses, where the thickness varies linearly with the interaction time. Under the rotating wave approximation (RWA), it is found that, if initially one of the modes is coherent and the other one squeezed, then the squeezing and non-Poissonianness of the photon statistics can be transferred from one mode to the other. It is shown that the transferred squeezing to the initially coherent mode is of new type. In that

mode the squeezed quadrature remains squeezed, whereas the other quadrature is antisqueezed throughout except at the points where both of them return to coherent value.

The squeezed angular momentum states, constructed from the conventional bosonic squeezed states, are found to be useful to decrease the minimum detectable phase difference of  $SU(2)$  interferometers. This eventually increase the accuracy of the interferometers. Gravitational waves, a long predicted disturbance and expected to be observed through a very accurate interferometer, produce very small path or phase difference in one of the arms with a heavy mass. In the last section, I apply the rotated SAMS state to estimate the minimum detectable phase and required parametric values for that. The results are compared with the previous estimates for different states.

The interaction of small number of trapped two-level atoms with coherent radiation are well studied[44]. The existing theory for the interaction of atoms with light waves adopted single particle density operator equation. In the fifth chapter, I apply the SAMC states to represent an ensemble of ultra cold two level bosonic atoms, connected by an allowed dipole transition. The Jaynes-Cummings[45] interaction of a coherent radiation with such an ensemble under RWA is considered in the perturbative framework. The frequency of the coherent radiation is assumed to be resonant with the spacing between the levels. The situation occurs when there are near condensates covering the recent experimentally achieved condensates[9–11]. Our results show generation of squeezing and other non-classical properties like non-Poissonian photon statistics of radiation, as expected from the previous study of such interaction with small number of atoms. The method also decreases the uncertainties of the AM quadratures representing the dipole vector of the atomic system. This opens up a possibility of generation of squeezed atomic states. The interaction also found to amplify the radiation without inverting the population difference.

The last chapter concludes the works presented in this thesis emphasizing the

main results. Some future extensions can be made of the current work providing better physical understanding. These extensions are also discussed in the last chapter.

## Chapter 2

# Coherent and squeezed states of harmonic oscillator

In this chapter I review the notion of coherent and squeezed states of the harmonic oscillator with some of their basic properties. I also present the physical systems, relevant for this thesis, represented by the coherent states.

### 2.1 Coherent states

The idea of coherent states was conceived way back in the year 1926 by Schrödinger in connection with classical states of quantum mechanical harmonic oscillator[5]. After a long dormant period, Glauber[2], Sudarshan[1] and Klauder[3] revived the interest in coherent states and extensively studied <sup>them</sup> in context of the radiation field. The development of the study of coherent states has been accompanied by the technical developments along with the invention of lasers. These are the states of classical nature originating from nearly quantum mechanical sources. In the following subsections I will discuss the basic definitions of the coherent states and some of their basic properties. The particles are assumed to be in a harmonic oscillator potential and follow Bose Einstein statistics. The bosonic particles, follow the commutation relation

$$[a, a^\dagger] = 1. \tag{2.1}$$

where  $a^\dagger$  and  $a$  are normalized creation and annihilation operators in the second quantized notation. Two orthogonal hermitian quadrature operators  $X$  and  $P$  can be constructed from the creation and annihilation operators

$$\begin{aligned} X &= \frac{1}{\sqrt{2}}(a^\dagger + a), \\ P &= \frac{1}{i\sqrt{2}}(a^\dagger - a). \end{aligned} \quad (2.2)$$

In terms of the conjugate operators, equation 2.2 reads as  $[X, P] = \hbar I$ . Finally the quadrature operators are connected to the observables for the two physical coherent systems of bosonic particles which are used in the thesis for application purpose.

### 2.1.1 Definitions of coherent states

Coherent states of harmonic oscillator can be defined in three ways. All the three mathematical definitions coincide for the case of single mode bosonic particles in harmonic oscillator potential.

*Definition 1: Annihilation Operator Coherent State (AOCS).* The coherent states  $|\alpha\rangle$  are eigenstates of the annihilation operator  $a$  of the harmonic oscillator,

$$a|\alpha\rangle = \alpha|\alpha\rangle, \quad \alpha = |\alpha|e^{i\theta}. \quad (2.3)$$

*Definition 2: Displacement Operator Coherent State (DOCS).* The coherent states  $|\alpha\rangle$  are the displaced states of the ground or vacuum state of the harmonic oscillator,

$$|\alpha\rangle = D(\alpha)|0\rangle, \quad D(\alpha) = \exp(\alpha a^\dagger - \alpha^* a). \quad (2.4)$$

$D(\alpha)$  is called the displacement operator.

*Definition 3: Minimum Uncertainty Coherent State (MUCS).* The coherent states  $|\alpha\rangle$  are quantum states with a minimum uncertainty relationship,

$$\Delta X \Delta P = \frac{1}{2}, \quad (2.5)$$

where  $(\Delta X)^2$  and  $(\Delta P)^2$  are the variances in the canonically conjugate self adjoint quadrature operators  $X$  and  $P$  of the harmonic oscillator when the matrix elements are calculated for the coherent states.

It is to be noted that the third definition is not unique. The so called *squeezed* states also qualify for this definition and so sometimes are called as *generalized coherent* states. These states are discussed in the next section of this chapter. However, only the states, with uncertainties in both the quadratures equal to the *standard quantum limit* (SQL)  $\frac{1}{\sqrt{2}}$ , are referred as coherent states in this thesis.

## 2.1.2 Properties of coherent states

With the above definitions the coherent states of the harmonic oscillator can be expressed in terms of Fock states and used as a set of continuous (in a complex plane), normalized, but non-orthogonal, and overcomplete basis states. This enables to express any arbitrary state in terms of coherent basis states. Further algebraic properties of these states are well studied and can be found in standard textbooks of quantum optics[4, 14]. The properties are liberally used in the calculation of the works presented in this thesis.

### 2.1.2.1 Fock state expansion of coherent states

Coherent states of harmonic oscillator can be expanded in the diagonal representation of Fock states or number states, the eigenstates of the oscillator hamiltonian as

$$|\alpha\rangle = e^{-\frac{1}{2}|\alpha|^2} \sum_0^{\infty} \frac{\alpha^n}{\sqrt{n!}} |n\rangle. \quad (2.6)$$

### 2.1.2.2 Non-orthogonality

By direct calculation using the Fock state expansion we get

$$|\langle\alpha|\alpha'\rangle|^2 = e^{-|\alpha-\alpha'|^2}. \quad (2.7)$$

The above relation shows that the coherent states are non-orthogonal.



### 2.1.2.3 Over-completeness and normalizability

Glauber[2] has shown that the resolution of the identity in terms of coherent states is not unique and a common resolution is

$$\frac{1}{\pi} \int d^2\alpha |\alpha\rangle \langle \alpha| = I. \quad (2.8)$$

As the coherent states are labeled by a continuous complex index in the Hilbert space that has a countable basis, they are over-complete. The above relation also shows that the coherent states can be normalized.

### 2.1.2.4 Coherent states as basis states

Using the overcompleteness property any arbitrary state can be expanded in terms of the coherent state basis as

$$|\psi\rangle = \frac{1}{\pi} \int |\alpha\rangle f(\alpha^*) e^{\frac{\alpha^2}{2}} d^2\alpha. \quad (2.9)$$

where the analytical function  $f(\alpha^*)$ , the coherent state representation of  $|\psi\rangle$ , is

$$f(\alpha^*) = \langle \alpha | \psi \rangle e^{\frac{\alpha^2}{2}} = \sum_n c_n \frac{(\alpha^*)^n}{\sqrt{n!}}. \quad (2.10)$$

### 2.1.2.5 Phase space diagram

The coherent states have the same Gaussian dependence on both the quadratures as of ground state of a harmonic oscillator but the mean is displaced by a constant amount  $|\alpha|$  from the zero value for the ground state. In the phase space diagram, in figure 2.1, the uncertainties of these states are represented by a circle around the mean position. The plots represent the uncertainties, quantitatively the full width at half maximum (FWHM) of the quasiprobability distribution function[14]. The circle at the origin is the uncertainty of the vacuum state, which has been displaced by an amount  $|\alpha|$  towards the angle  $\theta$ , the phase angle of the complex coherence parameter  $\alpha$ . The mean value of the quadratures rotate around the origin following the bigger circular path showing sinusoidal temporal dependence like a classical oscillator of same frequency.

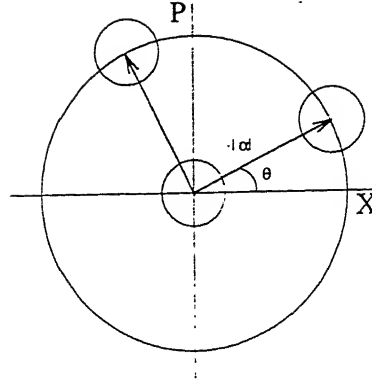


Figure 2.1: Phase space diagram of coherent and vacuum states of a harmonic oscillator.

### 2.1.3 Number statistics

The probability distribution of particles in a coherent state follows Poissonian statistics

$$P(n) = |\langle n|\alpha \rangle|^2 = |\alpha|^{2n} e^{-|\alpha|^2} / n! \quad (2.11)$$

where  $|\alpha|^2$  is the mean and variance of the particle number.

### 2.1.4 Physical systems represented by coherent states

Two types of coherent physical systems are considered, the coherent radiation field (a system of photons represented by above definitions) or laser, and coherently distributed ultra-cold bosonic atoms. The former one is responsible for the revival and most of the developments of the mathematical formulation of the coherent states. In the case of radiation, the vector potential, electric or magnetic fields as well as intensity are completely described by the creation and annihilation operators. The measured experimental observables are the quadratures of the electric field at  $\frac{\pi}{2}$  phase interval, which later are converted to the normalized quadratures  $X$  and  $P$ .

Though the development of coherent states followed the path of the optical

system, recent technological breakthrough succeeded in creating samples of atoms with thermal de Broglie wavelength comparable to the sample size, fulfilled at very low temperature and high densities. A careful look at the periodic table reveals that most of the atoms in their ground state are bosonic. During the last decade rapid progress has been made in the area of cooling and trapping of atoms. By combination of different cooling and trapping techniques the atoms could be kept at very low temperature ( $1-100 \mu\text{K}$ ) and high density ( $10^{10} - 10^{13} \text{ cm}^{-3}$ )[8]. More recently, further developed techniques has been reported to achieve Bose Einstein condensates (BEC) at densities  $10^{12} - 10^{14} \text{ cm}^{-3}$  and temperatures  $10^{-8} - 10^{-7}$  Kelvin in samples of rubidium[9], lithium[10] and sodium[11] atoms. At such low temperatures and high densities the atoms loose their individual identity and behave like a single macroscopic quantum state and the effect of quantum statistics becomes crucially important[12]. Such *ultra cold* atomic ensembles are expected to have properties similar to the role of lasers in conventional coherent optics[13]. Exploiting this analogy it is possible to express ultra cold samples as coherent state of harmonic oscillator. The quadratures represent dimensionless position and momentum of the atomic system.

## 2.2 Squeezed states

Though the concept of squeezed states has been first proposed by Yuen[15], in the name of *two photon* coherent states or *generalized* coherent states, the specific term *squeezing* came later[17–19]. The squeezed states of harmonic oscillator are the states defined in a similar line of way adopted in the definition of coherent states. These states have been first defined in context of light, but other systems have also been studied, though not comparably. All the definitions match with other for the single mode optical signal. However, we will see in the next chapter that there are discrepancies in the definition in other systems. The experimental production of squeezed states have reduced our uncertainty of observation to a non-classical sys-

tems. This enabled us to apply it for the technical uses of optical communication[23] and interferometry[20–22]as well as to understand some fundamental questions about quantum mechanics[14].

### 2.2.1 Definitions of squeezed states

The squeezed states of harmonic oscillator can be defined in three ways similar to the definition of coherent states. All the mathematical definitions coincide for the case of single mode radiation field.

*Definition 1: Two photon coherent state or generalized coherent state.* Yuen[15] has defined the generalized coherent states or the two photon coherent states  $|\beta\rangle$  as eigenstates of the operator  $b = \mu a + \nu a^\dagger$

$$b|\beta\rangle = \beta|\beta\rangle, \quad (2.12)$$

where  $\mu, \nu$  and  $\beta$  are in general complex numbers. The Bogoliubov transformation of  $a$  and  $a^\dagger$  to  $b$  and  $b^\dagger$  and the unitary generator for this transformation is discussed in the next definition.

*Definition 2: Squeezed vacuum or coherent state.* The squeezed states of harmonic oscillator  $|\beta\rangle = |\alpha, \xi\rangle$  are obtained by operating the squeezing operator

$$S(\xi) = \exp \frac{1}{2}(\xi a^{\dagger 2} - \xi^* a^2), \quad \xi = r e^{i\phi}, \quad (2.13)$$

on the coherent state  $|\alpha\rangle$ . If it is operated on the vacuum state, which is a special case of the coherent state with  $\alpha = 0$ , the resulting state is the squeezed vacuum. The Bogoliubov transformation is generated by operating the unitary squeezing operator on the annihilation and creation operator

$$b = S^{-1}(\xi)aS^{-1}(\xi), \quad b^\dagger = S^{-1}(\xi)a^\dagger S^{-1}(\xi). \quad (2.14)$$

The quantities  $\mu$  and  $\nu$  used in the previous definition is related to the squeezing parameter  $\xi$  as  $\mu = \cosh r$  and  $\nu = e^{i\phi} \sinh r$ . Fisher[46] have shown that the displacement and the squeezing operators do not commute but can be interchanged with dependencies on new parameters which are related to the older ones.

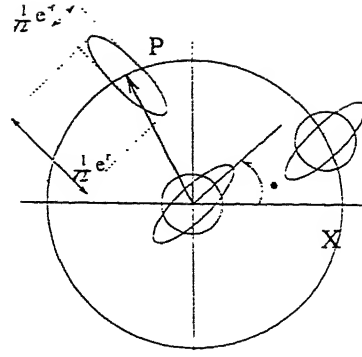


Figure 2.2: Phase space diagram of squeezed states of a harmonic oscillator.

*Definition 3: Uncertainty of any quadrature is less than the standard quantum limit (SQL). The squeezed states  $|\beta\rangle$  are quantum states having uncertainty in one of the quadratures less than that of the coherent or vacuum state, i.e.,*

$$\Delta X \text{ or } \Delta P < \frac{1}{2}. \quad (2.15)$$

but maintain the uncertainty relation. The first two definitions of squeezed states for the harmonic oscillator qualifies the third definition.

### 2.2.2 Phase space diagram

The phase space diagram of the squeezed states of harmonic oscillator is drawn in Fig. 2.2. The axes and the uncertainties are presented according to the same notation as in the case of coherent states. At the origin, the vacuum and the squeezed states are shown as the circle and the ellipse respectively. The squeezing deforms the uncertainty circle to an ellipse of axes lengths  $\frac{1}{\sqrt{2}}e^{\pm r}$ . The major axis makes an angle of  $\phi$  with the  $X$  axis. The squeezed states maintain the gaussian profile, for the coherent state wave function, with larger or smaller variance. The displaced or coherent and squeezed state is also shown in the diagram. It can be obtained either by displacing the squeezed vacuum or squeezing the coherent state. The time development of the squeezed state shows that the uncertainty of a certain quadrature oscillates as the ellipse rotates about its centre. However, the mean of the quadratures rotate in the same bigger circular path as before.

### 2.2.3 Number distribution

Unlike the coherent case, where the probability distribution follows Poissonian statistics, the squeezed states have variance in number larger or smaller than the mean value. I define the *statistics parameter*,  $\mathcal{B}$ , as

$$\mathcal{B} = \Delta n^2 - \langle n \rangle. \quad (2.16)$$

If  $\mathcal{B}$  is larger (smaller) than zero, the statistics shown by the system is called super-(sub-)Poissonian.

## Chapter 3

# Coherent and squeezed angular momentum states

Various types of coherent states have been defined for different type of physical systems, which include some generalization of harmonic oscillator coherent states. Angular momentum (AM) coherent states were also studied along with other physical systems. A good review of the group theoretical generalization of the coherent states is available in the review article[47], though several other text books are also available[4, 6]. One of the books[6]deals in detail the mathematical developments of the notion of so called coherent states suitable for different physical applications. In this thesis I will focus my interest in the field of angular momentum systems.

Apart from the intrinsic angular momentum systems, the AM algebra describes other physical pseudo-AM systems, namely, a)two mode radiation system, and, b)two level system. These states are of particular interest in quantum optics. Due to their binary structure, they are being investigated for quantum computation. Both the physical systems can be represented by the angular momentum algebra. The first system is described in the second section of this chapter, through the Schwinger representation of AM. The levels of a two level atom, taken into consideration for the rest of the work or molecule are assumed to be connected by dipole transition. The states denote the direction of the dipole vector or the Bloch vector in atomic physics paradigm. The Pauli matrices perfectly describe such a system. Though there is no

intrinsic physical AM involved, the systems follow the AM algebra. A collection of two level atoms can be represented by angular momentum algebra by adding up the individual *spins* of the atoms. The terms *level* and *mode* will be used equivalently in this thesis for the purpose of formulation.

The first section introduces the commutation relations and the uncertainty relations for the AM operators. The notion of squeezing for AM system is developed. The uncertainty relations followed by the AM operators and the phase angle are also presented. Though the coherent and squeezed states of single mode radiation is first to be studied over few decades, coherent and squeezed states of angular momentum systems have also been studied consequently during the early seventies. In the next section two definitions of AM coherent states[25, 26, 28] are presented and compared. The physical situations corresponding to both the definitions are mentioned. After the development in the generation of nonclassical radiation systems, some fundamental questions about coherent AM states were asked against one[25, 26] of the definitions in terms of squeezing. The other definition[28] is shown to be free from the ambiguity. This definition finds an application in the atomic system after the experimental generation of BEC[9–11], though well applied in two mode radiation.

In the last section, I extend the idea for coherent states of angular momentum in reference[28] to define the angular momentum squeezed states. I use the definition of the squeezing as any value of the uncertainty in a certain quadrature, in the left hand side of the uncertainty relation, less than it's value corresponding to the coherent state. It is shown that the states defined this section show squeezing in the AM space.



### 3.1 Uncertainty relations of angular momentum

AM operators follow the commutation relation between the components,  $[J_l, J_m] = i\epsilon_{lmn}J_n$ . Correspondingly the uncertainty relation followed by the AM operators is

$$\Delta J_l^2 \Delta J_m^2 \geq \frac{1}{4} |\langle J_n \rangle|^2. \quad (3.1)$$

which will be studied for  $l = x, m = y$  and  $n = z$ . Spin or AM systems are regarded to be squeezed if the uncertainty of a component, say  $\Delta J_x^2$  or  $\Delta S_y^2$  is smaller than  $\frac{1}{2} |\langle J_z \rangle|$  [31].

Carruthers and Nieto[48] pointed out that AM projection operator also obeys other uncertainty relations with the phase angle, following the commutation relations  $[J_z, S] = iC$  and,  $[J_z, C] = iS$ , are

$$\Delta J_z^2 \Delta S^2 \geq \frac{1}{4} \langle C \rangle^2, \quad \Delta J_z^2 \Delta C^2 \geq \frac{1}{4} \langle S \rangle^2. \quad (3.2)$$

The above relations can be combined to

$$\Delta J_z^2 (\Delta S^2 + \Delta C^2) \geq \frac{1}{4} (\langle S \rangle^2 + \langle C \rangle^2). \quad (3.3)$$

where, S and C are the sine and cosine operators of the phase defined in terms of two dimensional creation and annihilation operators as

$$\begin{aligned} \sin \Phi &= \frac{y_0(a_y^\dagger - a_y)}{[\{x_0(a_x^\dagger + a_x)\}^2 - \{y_0(a_y^\dagger + a_y)\}^2]^{\frac{1}{2}}} \\ \cos \Phi &= \frac{x_0(a_x^\dagger - a_x)}{[\{x_0(a_x^\dagger + a_x)\}^2 + \{y_0(a_y^\dagger + a_y)\}^2]^{\frac{1}{2}}}. \end{aligned} \quad (3.4)$$

following Susskind and Glogower[49].  $a_{x,y}$  and  $a_{x,y}^\dagger$  are annihilation and creation operators corresponding to the simple harmonic oscillators in the X and Y directions, with  $x_0$  and  $y_0$  as the amplitudes for the oscillators.

### 3.2 Angular momentum coherent states

In this section I will focus my interest in the two definitions of angular momentum coherent states developed in the early seventies. The definition in the first subsection

is due to two simultaneous works by Radcliffe[25] and Arecchi et al.[26]. I will refer these states as *coherent spin states* (CSS). CSSs describe states in a finite dimensional Hilbert space with fixed number of particles in the two levels or modes. The other definition, due to Atkins and Dobson (AD) using Schwinger bosonic representation of AM[28], is discussed in the next subsection. I will refer these states as *Schwinger angular momentum coherent* (SAMC) states. This representation spans an infinite dimensional AM Hilbert space, constructed from the infinite dimensional Hilbert spaces for the bosonic particles in the two modes or levels. The numbers of particles are not fixed, as in the case of CSS, but have some uncertainty. This creates a three dimensional structure of the uncertainty. SAMC states are compared with CSS to remove the ambiguity between coherent and squeezed AM states.

### 3.2.1 Coherent spin states

Coherent spin states (CSS) were independently defined by Radcliffe[25] and Arecchi et al.[26]. The definition of CSS is similar to the definition of field coherent states. Instead of displacement of the vacuum, as in the case of radiation, CSS are obtained by rotating the AM ground state. Radcliffe defined CSS as

$$|\mu\rangle = N^{-\frac{1}{2}} \exp(\mu J_-) |j, j\rangle = N^{-\frac{1}{2}} \sum_{m=0}^{2j} \left[ \frac{2j!}{p!(2j-p)!} \right] \mu^m |j, m\rangle. \quad (3.5)$$

The state is generated from the highest AM projection state. ACGT defined a rotation operator which introduces a rotation through an angle  $\theta$  about an axis  $\hat{n} = (\sin \phi, -\cos \phi, 0)$  as shown in figure 3.2.1

$$R_{\theta, \phi} = e^{-i\theta J_n} = e^{-i\theta(J_x \sin \phi - J_y \cos \phi)} = e^{\zeta J_+ - \zeta^* J_-}, \quad (3.6)$$

where  $\zeta = \frac{1}{2}\theta \exp(-i\phi)$ . CSS, which he refers as *atomic coherent states* or *Bloch states* is obtained by rotation of the ground state  $|j, -j\rangle$

$$|\theta, \phi\rangle = R_{\theta, \phi} |j, -j\rangle. \quad (3.7)$$

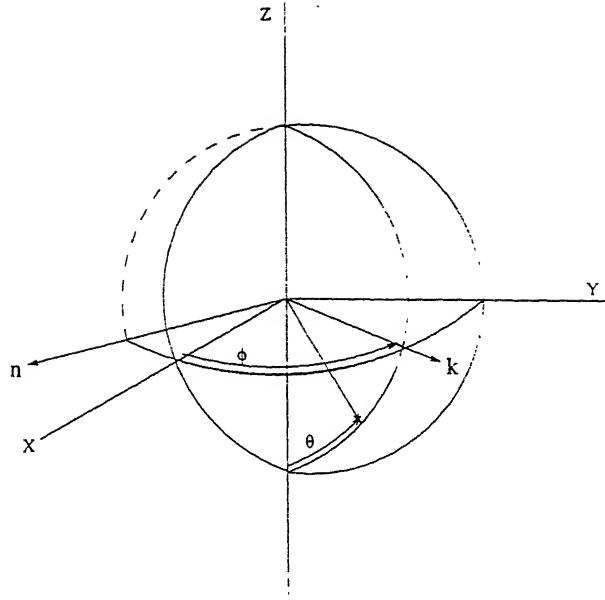


Figure 3.1: The rotation caused by the rotation operator defined in equation 3.6 .

In fact the rotation operator, defined by ACGT, can generate CSS from the highest weighted state also. This is due to the consideration of complete rotation operator used by ACGT. The observation also points to the SU(2) symmetry of the system.

Referring to figure 3.1, it is seen that,

$$\begin{aligned}
 R_{\theta,\phi} J_n R_{\theta,\phi}^{-1} &= J_n \\
 R_{\theta,\phi} J_k R_{\theta,\phi}^{-1} &= J_k \cos \theta + J_z \sin \theta \\
 R_{\theta,\phi} J_z R_{\theta,\phi}^{-1} &= -J_k \sin \theta + J_z \cos \theta
 \end{aligned} \tag{3.8}$$

where,  $J_n = J_x \sin \phi - J_y \cos \phi$ , and,  $J_k = J_x \cos \phi + J_y \sin \phi$ , which gives,

$$J_+ = (J_k - iJ_n)e^{i\phi}, \quad J_- = (J_k + iJ_n)e^{-i\phi} \tag{3.9}$$

Using the above relations, one obtains

$$R_{\theta,\phi} J_- R_{\theta,\phi}^{-1} = e^{-i\phi} \left[ J_- e^{i\phi} \cos^2 \frac{\theta}{2} - J_+ e^{-i\phi} \sin^2 \frac{\theta}{2} + J_z \sin \theta \right]$$

$$\begin{aligned}
R_{\theta,\phi} J_+ R_{\theta,\phi}^{-1} &= e^{i\phi} [J_+ e^{-i\phi} \cos^2 \frac{\theta}{2} - J_- e^{i\phi} \sin^2 \frac{\theta}{2} + J_z \sin \theta] \\
R_{\theta,\phi} J_z R_{\theta,\phi}^{-1} &= J_z \cos \theta - \frac{1}{2} \sin \theta [e^{i\phi} J_- + e^{-i\phi} J_+]
\end{aligned} \tag{3.10}$$

From the last equation and the definition of CSS, one obtains the eigenvalue equation

$$[J_- e^{i\phi} \cos^2 \frac{\theta}{2} - J_+ e^{-i\phi} \sin^2 \frac{\theta}{2} + J_z \sin \theta] |\theta, \phi\rangle = 0 \tag{3.11}$$

This equation, together with  $J^2 |\theta, \phi\rangle = J(J+1) |\theta, \phi\rangle$ , specifies the CSS uniquely.

Other forms of the eigenvalue equation can be obtained using the relation  $R_{\theta,\phi} J_z R_{\theta,\phi}^{-1} |\theta, \phi\rangle = -J |\theta, \phi\rangle$ , and the transformation relation of  $J_z$  under rotation. The resulting equation can be combined with the last equation to eliminate one of the operators  $J_z$ ,  $J_+$ , or  $J_-$ , giving

$$\begin{aligned}
\left[ J_- e^{i\phi} \cos^2 \frac{\theta}{2} + J_+ e^{-i\phi} \sin^2 \frac{\theta}{2} \right] |\theta, \phi\rangle &= J \sin \theta |\theta, \phi\rangle, \\
\left[ J_- e^{i\phi} \cos \frac{\theta}{2} + J_z \sin \frac{\theta}{2} \right] |\theta, \phi\rangle &= J \sin \frac{\theta}{2} |\theta, \phi\rangle, \\
\left[ J_+ e^{-i\phi} \sin \frac{\theta}{2} + J_z \cos \frac{\theta}{2} \right] |\theta, \phi\rangle &= J \cos \frac{\theta}{2} |\theta, \phi\rangle.
\end{aligned} \tag{3.12}$$

These additional relations are not independent of the eigenvalue equations mentioned earlier.

Using disentangling theorem for AM operators[26], the rotation operator,  $R_{\theta,\phi}$ , becomes

$$R_{\theta,\phi} = e^{-\tau^* J_-} e^{-\ln(1+|\tau|^2) J_z} e^{\tau J_+} = e^{\tau J_+} e^{\ln(1+|\tau|^2) J_z} e^{-\tau^* J_-}, \tag{3.13}$$

where,  $\tau = e^{-i\phi} \tan \frac{\theta}{2}$ . The last form of the above equation, which is normally ordered, immediately gives the expansion of  $|\theta, \phi\rangle$  in terms of Dicke states or the AM projection eigenstates,

$$\begin{aligned}
\langle j, m | \theta, \phi \rangle &= \binom{2j}{j+m}^{\frac{1}{2}} \frac{\tau^{j+m}}{[1+|\tau|^2]^j} \\
&= \binom{2j}{j+m} \sin^{j+m} \frac{\theta}{2} \cos^{j-m} \frac{\theta}{2} e^{-i(j+m)\phi}.
\end{aligned} \tag{3.14}$$

The overlap of two CSS is obtained from the above equation, using completeness property of Dicke states, as

$$\begin{aligned} \langle \theta, \phi | \theta', \phi' \rangle &= \left[ \frac{(1 + \tau^* \tau')^2}{(1 + |\tau|^2)(1 + |\tau'|^2)} \right]^j \\ &= e^{ij(\phi - \phi')} \left[ \cos \frac{\theta - \theta'}{2} \cos \frac{\phi - \phi'}{2} - i \cos \frac{\theta + \theta'}{2} \sin \frac{\phi - \phi'}{2} \right]^{2j}. \end{aligned} \quad (3.15)$$

whence  $|\langle \theta, \phi | \theta', \phi' \rangle|^2 = \cos^{4j} \frac{\Theta}{2}$ , where  $\Theta$  is the angle between the directions of the two states, given by  $\cos \Theta = \frac{1}{4} \sin 2\theta \sin 2\theta' \cos(\phi - \phi')$ .

The CSSs are minimum uncertainty packets. The uncertainty relation can be defined in terms of the rotated operators  $(J_x, J_y, J_z) = R_{\theta, \phi} (J_x, J_y, J_z) R_{\theta, \phi}^{-1}$ . It is easy to show that the equality holds in the uncertainty relation  $\Delta J_x^2 \Delta J_y^2 \geq \frac{1}{4} |J_z|^2$ , but not equation 3.1. The symmetry properties were also studied by ACGT and compared with the harmonic oscillator.

The CSS and the operators involved in their description, further obey a number of properties : (i) the states are nonorthogonal like harmonic oscillator coherent states; (ii) AM operators obey a large number of Baker-Campbell-Housedorff formulae; (iii) within a fixed Bloch subspace the statistical operators have a diagonal representation in the coherent state representation. The state has no uncertainty in the length of the AM vector as they are rotated eigenstates of square of total AM operator and AM projection operator.

Agarwal[50] established the relationship between CSS and the state multipoles, using the multipole operator definition[51]

$$T_{KQ} = \sum_{m=-j}^j \sum_{m'=-j}^j (-)^{j-m} \sqrt{2K+1} \begin{pmatrix} j & K & j \\ -m & Q & m' \end{pmatrix} |j, m\rangle \langle j, m'| \quad (3.16)$$

with  $T_{KQ}^\dagger = (-)^Q T_{K-Q}$ . The state multipoles were used to develop a theory of generalised phase space description of AM systems. Dowling et al.[52] calculated the Wigner distribution for CSS using the work of Agarwal. A. Vaglica and G. Vetri[53] have shown that AM projection and phase angle uncertainties reach minimum at classical (large  $j$ ) limit. The physical radiation system corresponding to the eigenstates of AM projection, of which CSSs are a subset, are two mode pure number

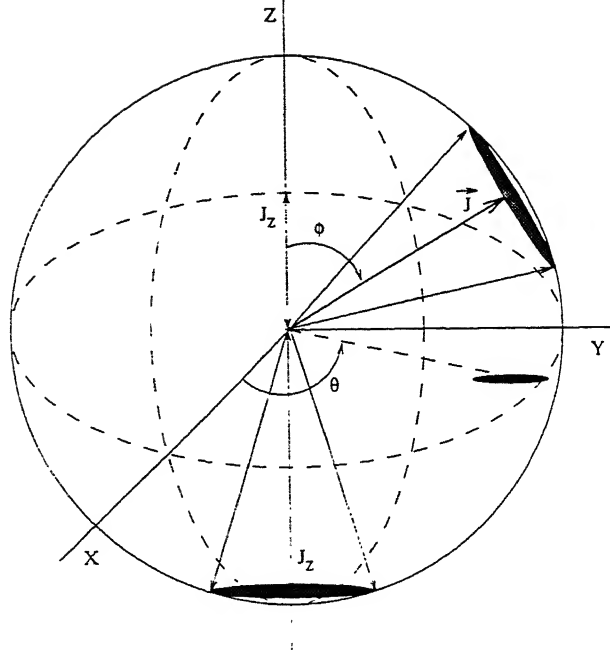


Figure 3.2: The rotation of CSS generates SSS. Notice the projection of the CSS on X-Y plane.

state. These states are yet to be produced experimentally. The corresponding atomic picture is much clear, where fixed number of atoms can be confined experimentally in a trap.

It has been pointed out by Kitagawa and Ueda[29] that the definition of spin squeezing, as in the previous section, implies that a CSS is already squeezed if it is placed in appropriate coordinate system, and also that spin can be squeezed by just rotating CSS as described in figure 3.2. But the rotation or  $SU(2)$  transformation is a subgroup of the *passive*  $U(2)$  group. With other *active* quadratic elements, the  $U(2)$  subgroup forms the complete  $Sp(4, \mathbb{R})$  group to describe all two mode quadratic transformations[32]. The active elements introduce further squeezing in the system but the passive elements effectively keeps the parameters, defining the degree of squeezing, unchanged. Squeezed light emission from an atomic system in a certain CSS[54] has been regarded as evidence justifying the definition of squeezing of AM operators. However, it is by no means obvious that one can judge the squeezing of

spin by referring to the uncertainty of another (photon) system interacting with it.

### 3.2.2 Angular momentum coherent states in Schwinger representation

Atkins and Dobson (AD) defined the coherent AM states using the Schwinger bosonic representation for AM operators[28]. In this subsection, I present the definition of these states and compare them with the CSS. The definition does not show the ambiguity of being squeezed by a mere rotation.

#### 3.2.2.1 Schwinger angular momentum algebra

Schwinger[33] developed the entire angular momentum algebra in terms of two sets(up and down) of uncorrelated harmonic oscillator creation and annihilation operators constructing the angular momentum operators as

$$\begin{aligned} J_+ &= J_x + iJ_y = a_+^\dagger a_- \\ J_- &= J_x - iJ_y = a_-^\dagger a_+ \\ J_z &= \frac{1}{2}(a_+^\dagger a_+ - a_-^\dagger a_-). \end{aligned} \quad (3.17)$$

The operators  $a_\pm^\dagger(a_\pm)$  create (annihilate) a  $\pm\frac{1}{2}$  spin and follow the bosonic commutation relations which means the whole system is considered as a combination of two sets of boson states. The construction satisfies the standard angular momentum commutation relation  $[J_l, J_m] = i\epsilon_{lmn}J_n$ .

The total number operator, important for the interferometric purpose, is the sum of the two( $\hat{n}_\pm$ ) number operators

$$\hat{N} = \hat{n}_+ + \hat{n}_- = (a_+^\dagger a_+ + a_-^\dagger a_-) \quad (3.18)$$

The length of the AM vector is half of the expectation value of the total number operator.

The angular momentum basis states  $|j, m\rangle$  can be created by action of the oscillator operators on the vacuum spinor  $|0, 0\rangle$  as,

$$|j, m\rangle = |j + m\rangle_+ \oplus |j - m\rangle_- = [(j + m)!(j - m)!]^{-\frac{1}{2}} (a_+^\dagger)^{j+m} (a_-^\dagger)^{j-m} |0, 0\rangle \quad (3.19)$$

with  $j = \frac{1}{2}(n_+ + n_-)$  and  $m = \frac{1}{2}(n_+ - n_-)$ .

### 3.2.2.2 Schwinger angular momentum coherent states

AD[28] constructed the *Schwinger angular momentum coherent* (SAMC) states as the simultaneous eigenstates of the operators  $a_\pm$ . It is shown that the SAMC states are minimum uncertainty states for the angular momentum-angle uncertainty relation in the large  $N$  ( $N = n_+ + n_- \geq 10$ ) limit[28]. According to the definition of AD, the angular momentum coherent states  $|\tilde{\alpha}\rangle = \tilde{D}|0, 0\rangle$ , with  $\tilde{D} = D_+(\alpha_-)D_-(\alpha_-)$ , obey,

$$a_\pm |\tilde{\alpha}\rangle = a_\pm |\alpha_+, \alpha_-\rangle = \alpha_\pm |\alpha_+, \alpha_-\rangle. \quad (3.20)$$

The expansion of  $|\tilde{\alpha}\rangle$  in terms of angular momentum basis is given by

$$|\tilde{\alpha}\rangle = e^{-\frac{1}{2}N} \sum_{j=0}^{\infty} \sum_{m=-j}^j (2j!)^{-\frac{1}{2}} \binom{2j}{j+m}^{\frac{1}{2}} \alpha_+^{j+m} \alpha_-^{j-m} |j, m\rangle. \quad (3.21)$$

Following the multipole expansion procedure due to Agarwal[50], any arbitrary operator can be expanded in terms of state multipoles  $T_{KQ}$ . For the case of SAMC states, the coefficients of the density operator can be written in terms of labeled density operators as  $\rho_{KQ} = \sum_{j=0}^{\infty} \rho_{KQ}^j$ , as the transitions between two  $j$  levels is forbidden. The labeled density operators can further be written in terms of state multipoles with the coefficients reading as

$$\begin{aligned} \rho_{KQ}^j &= Tr[\hat{\rho} T_{KQ}^\dagger] = (-)^Q \sqrt{2K+1} e^{-N} \\ &\times Tr \left[ \sum_{m, m', m''=-j}^j (-)^{j-m'} i \frac{\alpha_+^{2j+m+m'}}{[(j+m)!(j+m')!]^{\frac{1}{2}}} \frac{\alpha_-^{2j-m-m'}}{[(j-m)!(j-m')!]^{\frac{1}{2}}} \right. \\ &\times \left. \begin{pmatrix} j & K & j \\ -m' & Q & m'' \end{pmatrix} |j, m\rangle \langle j, m''| \right] \end{aligned} \quad (3.22)$$



The  $\infty:1$  mapping of  $\tilde{\alpha}$  onto  $(\langle J_x \rangle, \langle J_y \rangle, \langle J_z \rangle)$  is a consequence of the 2:1 homomorphism of SU(2) and SO(3)[55]. SU(2) is spanned by the subset of spinors of length  $\sqrt{N}$  and SO(3) is spanned by the subset of vectors of length  $\langle J \rangle$ . The spinor  $|\tilde{\alpha}\rangle$  is a vector sum of different vectors  $|j, m\rangle$  in the physical angular momentum space. Once the four parameters in  $\alpha_{\pm}$  are fixed, it automatically fixes the values of  $j$  and  $m$  in the AM space. To calculate the mean and variances of the angular momentum components one has to use their expressions in SAMC state basis and fix the corresponding parameters. The matrix elements can be expressed in terms of any set of these parameters ( $\alpha_{\pm}$  or  $j$  and  $m$ ). The expressions in terms of the AM parameters give better understanding in the physical space. For this reason the matrix elements are expressed in terms of angular momentum parameters.

The mean of the angular momentum components are calculated as

$$\begin{aligned}\langle J_x \rangle &= \sqrt{j^2 - m^2} \cos \Theta \\ \langle J_y \rangle &= \sqrt{j^2 - m^2} \sin \Theta \\ \langle J_z \rangle &= m\end{aligned}\tag{3.23}$$

where  $\Theta = (\theta_+ - \theta_-)$  and the variances are

$$\Delta J_x^2 = \Delta J_y^2 = \Delta J_z^2 = \frac{1}{2}j\tag{3.24}$$

The above results show that the average value of  $\vec{J}$  i.e. the its tip lies on a sphere of radius  $j$ . The fluctuations of the components are also same in the three directions. The equation of the region of uncertainty creates a sphere of radius  $\sqrt{\frac{3j}{2}}$  about the tip of the vector. This is schematically shown in Fig. 3.3. The polar angle of the state vector in the three dimensional phase space is realized to be  $\Theta$ , the difference between two phase angles of the coherence parameters.

In three dimensional phase space we have the uncertainty sphere of the angular momentum vector in figure (3.3). This can be compared with the uncertainty circle of the harmonic oscillator in two dimensional phase space in the figure 2.1. For SAMC states the radii of the uncertainty spheres ( $= \sqrt{\frac{3j}{2}}$ ) depends only on the length of  $\vec{J}$ ,

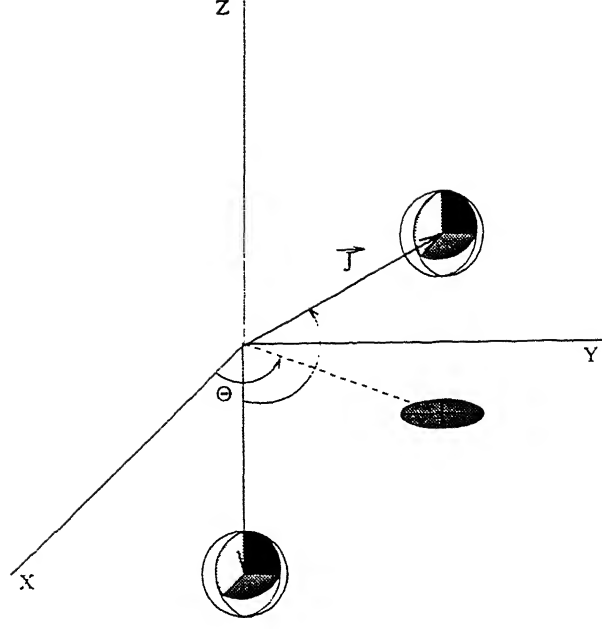


Figure 3.3: The phase space diagrams for SAMC states in two directions are shown. The projection of the uncertainty sphere on X-Y plane is always circular.

For a fixed  $j$  value the radii of the uncertainty spheres does not vary on its position on the sphere for the choice of the parameters  $m$  or  $\Theta$ . The uncertainty spheres has a circular projection (uncertainty circle) in the X-Y plane. It is to be noted that the uncertainty circle does not vary under rotation. So the problem of squeezing under rotation does not arise. This property allows SAMC states to qualify as AM coherent states better than CSS. The uncertainty sphere for rotated SAMC state is also shown in the same figure. The positions for  $|m| < j$  can be compared with the displacement of the ground state in the phase space picture for harmonic oscillator. The displacement of the uncertainty circle in the phase space of harmonic oscillator is performed by the rotation of the uncertainty sphere in corresponding three dimensional phase space for SAMC states. The position after rotation is governed by the values of the parameters  $m$  and  $\Theta$ .

Putting the expressions of the matrix elements for SAMC states in the equation 3.1 one can check that the equality occurs at  $m = \pm j$ . Two solutions for the equality project the SU(2) symmetry of the system. Other values of the angular momen-

tum projection have uncertainties of both the quadratures equal and same as the extremum cases. Though the non-extremum cases does not violate the uncertainty relation in the last equation but the relation is an equality only for extremum cases. Anyway, for physical purposes we are interested in the absolute uncertainties in the quadratures which remain same for all the SAMC states with same  $j$  value.

### 3.3 Angular Momentum Squeezed States

Defining AM squeezed states is the obvious extension to coherent AM states. There was a proposal to generate AM squeezing by correlating the individual spins through quadratic interaction. The interaction Hamiltonians considered are (i) *one axis twisting* :  $\propto J_z^2$ , and, (ii) *two axis twisting* :  $\frac{\hbar\lambda}{2i}(J_+^2 - J_-^2)$ . In this section I construct the AM squeezed states using Schwinger representation and show that they show squeezing property.

Following the work of AD on angular momentum coherent states, I have generated squeezed angular momentum states by operating the squeezing operators of the bosonic states on the SAMC states. For the two mode ( $\pm$ ) bosonic case the squeezing operators can be defined as

$$S_{\pm}(\xi_{\pm}) = \exp\left[\frac{1}{2}(\xi_{\pm}a_{\pm}^{\dagger 2} - \xi_{\pm}^*a_{\pm}^2)\right], \quad \xi_{\pm} = r_{\pm}e^{i\phi_{\pm}}. \quad (3.25)$$

I have created the general SAMS states by operating the two mode squeezing operator  $\tilde{S} = S_+(\xi_+)S_-(\xi_-)$  on the SAMC states

$$|\psi\rangle = S_+(\xi_+)S_-(\xi_-)D_+(\gamma_+)D_-(\gamma_-)|0,0\rangle \quad (3.26)$$

For convenience in calculation I use the relation to interchange the order of the squeezing and displacement operators[46] and write the general SAMS states as

$$|\psi\rangle = D_+(\alpha_+)D_-(\alpha_-)S_+(\xi_+)S_-(\xi_-)|0,0\rangle \quad (3.27)$$

where  $\gamma_{\pm} = \cosh r_{\pm}\alpha_{\pm} + e^{i\phi_{\pm}} \sinh r_{\pm}\alpha_{\pm}^*$ .

### 3.3.1 Single mode squeezing

The calculation of the expectation values and variances of the operators of our interest is cumbersome due to the dependence on the large number (eight) of parameters involved in the general SAMS states. For simplicity one of the squeezing operators is dropped to squeeze only one mode. The practical reasoning for this choice will be given in the next subsection. The SU(2) symmetry tells that one can choose any one of the two modes for squeezing. The squeezing for one mode can be obtained from the results of squeezing in the other mode just by interchanging the suffices. I choose to squeeze only in the + mode and the expression of the basis state vectors of single mode SAMS states are reduced to

$$|\psi\rangle = \tilde{D}S_+(\xi_+)|0,0\rangle. \quad (3.28)$$

The expectation and variance of the AM operators are calculated to be (see Appendix)

$$\begin{aligned} \langle J_x \rangle &= \Re(\alpha_+ \alpha_-^*), \\ \langle J_y \rangle &= \Im(\alpha_+ \alpha_-^*), \\ \langle J_z \rangle &= m + \frac{1}{2} \sinh^2 r. \end{aligned} \quad (3.29)$$

and,

$$\begin{aligned} \Delta J_x^2 &= \frac{1}{2}j + \frac{1}{2} \sinh r \left[ \frac{1}{2} \sinh r \{1 + 2(j - m)\} + (j - m) \cosh r \cos \delta \right], \\ \Delta J_y^2 &= \frac{1}{2}j + \frac{1}{2} \sinh r \left[ \frac{1}{2} \sinh r \{1 + 2(j - m)\} - (j - m) \cosh r \cos \delta \right], \\ \Delta J_z^2 &= \frac{1}{4} |\alpha_+|^2 [e^{2r} \cos^2 \eta + e^{-2r} \sin^2 \eta] + \frac{1}{2} \sinh^2 r \cosh^2 r - \frac{1}{4} |\alpha_-|^2. \end{aligned} \quad (3.30)$$

where  $\langle X \rangle = \langle \psi | X | \psi \rangle$ ,  $\Delta X^2 = \langle \psi | X^2 | \psi \rangle - \langle \psi | X | \psi \rangle^2$ , with  $\eta = \theta_+ - \frac{\phi}{2}$  and  $\delta = 2\theta_- - \phi$ .  $\theta_{\pm}$  are the phase angle of  $\alpha_{\pm}$  while  $r$  and  $\phi$  are the squeezing parameters of the + mode, without the unnecessary suffix.  $j$  and  $m$  are the expectation values of  $\frac{1}{2}(\hat{n}_+ \pm \hat{n}_-)$  without squeezing. It is noticed that the squeezing has no effect on the

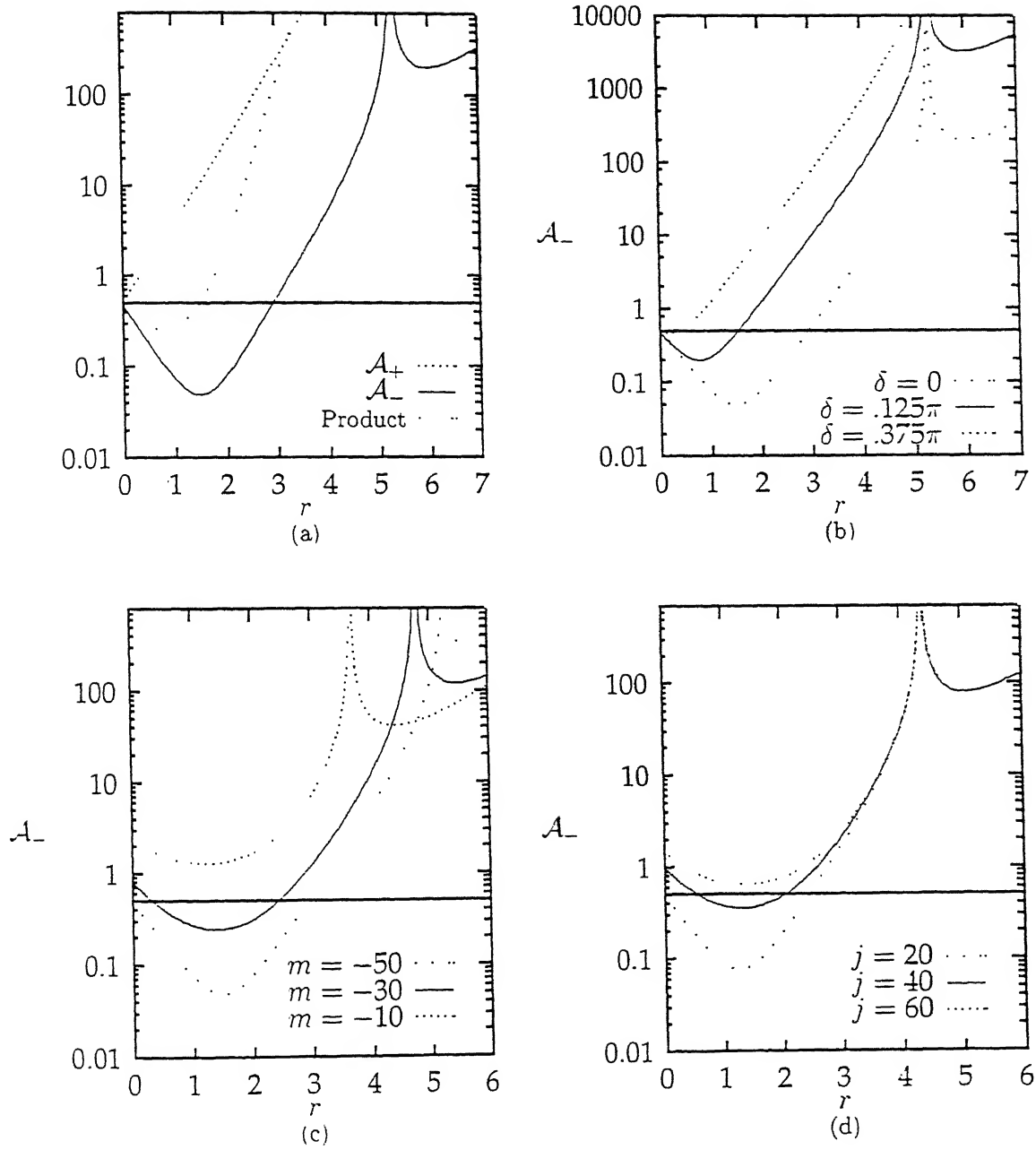


Figure 3.4: Parametric dependences of the quadratures. (a) Variation of  $\mathcal{A}_+$ ,  $\mathcal{A}_-$  and their product *w.r.t.*  $r$  for  $j = 50$ ,  $m = -50$  and  $\delta = 0$ . (b) Variation of  $\mathcal{A}_-$  with  $r$  for different  $\delta$  with  $j = 50$ ,  $m = -50$ . (c) Variation of  $\mathcal{A}_-$  with  $r$  for  $j = 50$ ,  $\delta = 0$  and  $m = -50, -30, -10$ . (d) Variation of  $\mathcal{A}_-$  with  $r$  for  $m = -20$ ,  $\delta = 0$  and  $j = 20, 40, 60$ .

mean values of  $J_x$  and  $J_y$  [28]. The effect of squeezing on  $\Delta J_z$  is clear from the last equation.

From equations 3.1 and the last one it is noticed that one needs to study the behavior of the two normalized quadratures calculated as

$$\begin{aligned}\mathcal{A}_+ &= \frac{\Delta J_x^2}{|\langle J_z \rangle|} = \frac{1}{2} \frac{-j + \sinh r [\frac{1}{2} \sinh r \{1 + 2(j - m)\} + (j - m) \cosh r \cos \delta]}{|m + \frac{1}{2} \sinh^2 r|}, \\ \mathcal{A}_- &= \frac{\Delta J_y^2}{|\langle J_z \rangle|} = \frac{1}{2} \frac{-j + \sinh r [\frac{1}{2} \sinh r \{1 + 2(j - m)\} - (j - m) \cosh r \cos \delta]}{|m + \frac{1}{2} \sinh^2 r|}\end{aligned}\quad (3.31)$$

and their product with change of parameters  $j, m, \delta$  and  $r$ . The quadratures show a singularity at  $\sinh^2 r = -2m$  due to the denominator and varies linearly on  $j$  whereas inversely on  $m$ . The cosine dependence term on  $\delta$  produces the difference in two quadratures showing no squeezing at  $\delta = (2n + 1)\frac{\pi}{2}$  and maximum squeezing (if it is there) at  $\delta = n\pi$ . The no squeezing line is the symmetry line of squeezing of the two quadratures *i.e.*  $\mathcal{A}_+$  is squeezed in the region  $\frac{\pi}{2} < \delta < \frac{3\pi}{2}$  and  $\mathcal{A}_-$  is squeezed in  $-\frac{\pi}{2} < \delta < \frac{\pi}{2}$ . The cosine dependence also shows symmetry between second and third quadrants of  $\delta$  for  $\mathcal{A}_+$  and between first and fourth quadrant for  $\mathcal{A}_-$  squeezing. This allows us to concentrate on the  $\delta$  dependence only in the first quadrant.

The dependence of  $\mathcal{A}_\pm$  on  $r$  is not simply exponential as in the case of phase space squeezing of bosons. I have studied the dependence of  $\mathcal{A}_\pm$  numerically as a function of  $\delta, j, m$  and  $r$ . These results are shown in figure 3.4. The vertical scales are taken to be logarithmic. The thick horizontal lines are drawn at the numerical value of 0.5. The SAMS states are squeezed within the range  $r_1 < r < r_2$  below this line. The numerical values of  $r_i (i = 1, 2)$  depend on all other parameters  $\delta, m$  and  $j$ . In all cases maximum squeezing is observed at  $m = -j$  and  $\delta = 0$ .

In figure 3.4(a) I have plotted  $\mathcal{A}_\pm$  and their product as a function of  $r$  with  $j = 50, m = -50$  and  $\delta = 0$ . The striking observation from the behavior of the product is that the SAMS states are no longer minimum uncertainty state for  $r > 0$ . The limiting condition  $r = 0$  reduces to the special case of SAMC states and  $r > 0$  includes the squeezing domain. In bosonic case the squeezed states are always minimum uncertainty states *i.e.* a subset of minimum uncertainty states. As mentioned before,

two quadratures  $\mathcal{A}_{\pm}$  are symmetric and can be interchanged by putting  $\delta = \pi$  in this plot. Due to this symmetry I concentrate to study only  $\mathcal{A}_{-}$  in figures 3.4b-d.

In figure 3.4(b) I have studied the dependence of  $\mathcal{A}_{-}$  on  $r$  for specific values of  $\delta$  with  $j = 50$  and  $m = -50$ . It is observed that an increase in  $\delta$  shifts both the minima upwards allowing less range of  $r$  for squeezing. As a consequence the value of upper bound of  $r$  for squeezing is decreased. It also shifts the minimum in the squeezing region towards lower values of  $r$ . At a constant value of  $\delta = \delta_c$  (which obviously depends on other parameters) the squeezing disappears. The plots remain unchanged as  $\delta \rightarrow -\delta$ . However, as  $\delta \rightarrow \delta + \frac{\pi}{2}$  then  $\mathcal{A}_{-}$  is replaced by  $\mathcal{A}_{+}$ .

The variation of  $\mathcal{A}_{-}$  with  $r$  for different values of  $m$  is shown figure 3.4(c). Increase in  $m$  value shifts the first minimum upwards as  $m$  is varied from -50 to -10 in steps of 20. From our numerical results it is observed that there is no squeezing in the region  $m \geq -\frac{j}{4}$ . The location of the singularity clearly depends on  $m$ . However, the second minimum does not follow the behavior of the first one. The numerical value of it decreases a little but nowhere near that of squeezing. From the figure it is seen that the second minimum occurs at lower values of  $r$  as  $m$  increases. Variations of  $\mathcal{A}_{-}$  with  $r$  for a fixed value of  $m = -20$  and  $j = 20, 40, 60$  are plotted in figure 3.4(d). Maximum squeezing is observed at  $j = 20$  and  $m = -20$ . For higher values of  $j$  i.e.  $m > -j$  the squeezing observed is reduced. It is also observed that the range of  $\delta$  for squeezing increases with an increase in  $j$  while the  $m$  value is kept fixed.

The uncertainty ellipsoid for  $m = -j$  have been shown in figure (3.6). It is to be noted that all the axes of this uncertainty ellipsoid are different. This results to an elliptical projection on the X-Y plane. The squeezing of angular momentum can be compared with the harmonic oscillator squeezing. In the same figure I have shown the dependence of the axes of the projected uncertainty ellipses on the squeezing parameter  $r$ . The projected uncertainty circle on the X-Y plane for the SAMC states are transformed to ellipses, but with greater area (uncertainty product). It is clear from the expressions that the maximum squeezing i.e. minimum fluctuation of the squeezed quadrature occurs to the minimum uncertainty circle at

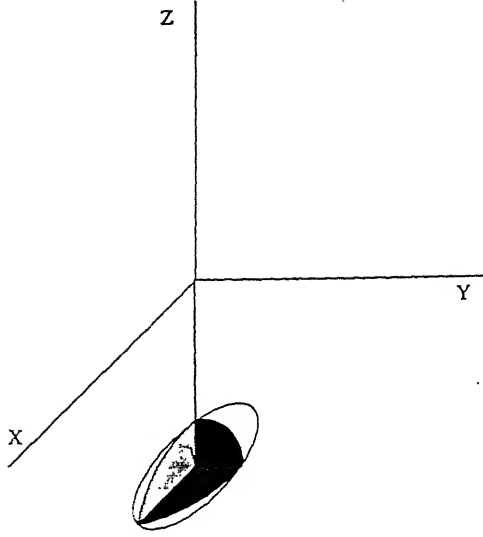


Figure 3.5: Schematic phase space diagram of SAMS state at pole.

$m = \pm j$  as expected physically. The minimum uncertainty circle is squeezed (length of the semiminor axis is reduced) up to a critical value of  $r$  ( $=r_{min}$ ) though its area (uncertainty product) is increased throughout. After that critical value of  $r$  the length of both the axes of the uncertainty ellipse increases.

It is interesting to note that squeezing in the + or - mode results squeezing of uncertainty in  $J_y$  and  $J_x$  respectively. This means that the squeezing in the angular momentum quadratures are directly related to the mode of squeezing. It will be interesting to express the squeezing operators in terms of operators in X-Y coordinates instead of  $\pm$  to identify the reason and exact mapping between them. The angle quadrature corresponding to the angular momentum needs some physical understanding in the context of two dimensional harmonic oscillators. Nieto[48] had developed a procedure to treat the oscillators in  $\pm$  basis as created from two oscillators quantized in the X and Y directions. To follow his prescription, one has to express the squeezing operator in X-Y basis. This creates some disentanglement problem. The problem can be handled by putting certain constraints on the parameters. It does not arise in the case of SAMC states. The connection between SAMC



states and coherent states of two dimensional oscillator is trivial[28], which is not so for SAMS states. The physical constraints for the disentanglement problem may show interesting properties.

### 3.3.2 Double mode squeezing

In the last subsection I have squeezed only in one mode for the sake of simplicity and promised to give the practical reasoning for this simplification in this subsection. Actually two mode squeezing does not help in reducing the uncertainty of any of the quadratures which we will show now. We can claim from the results of the last subsection that if we squeeze both the modes the uncertainties of the quadratures will be squeezed and expanded simultaneously. The squeezing of the second mode in effect reduce the amount of squeezing achieved by the first mode squeezing.

I have calculated the expectation values of the components of the angular momentum for double mode squeezing for real squeezing parameters as

$$\begin{aligned}\langle J_x \rangle &= \sqrt{j^2 - m^2} \cos \Theta, \\ \langle J_y \rangle &= \sqrt{j^2 - m^2} \sin \Theta, \\ \langle J_z \rangle &= m + \frac{1}{2}(\sinh^2 r_+ - \sinh^2 r_-).\end{aligned}\tag{3.32}$$

The expectations of the angular momentum components in X and Y direction are seen to be same as that of SAMC states with no effect of squeezing. The length of the AM vector will increase or decrease as difference of squares of the hyperbolic sine functions of the two parameters  $r_{\pm}$ . However, the expectation value of  $J_z$  can be made to be same as that of SAMC states by squeezing both the modes equally. This will make the length of the AM vector to be same as for SAMC states.

To show that the effect of double mode squeezing does not help in squeezing of the angular momentum quadratures I have calculated the uncertainties for some special choice of parameters. I have chosen the phases in the squeezing parameters to be equal to zero. This choice does not affect the basic motivation of proving the disadvantage of double mode squeezing. I have calculated the uncertainties in the

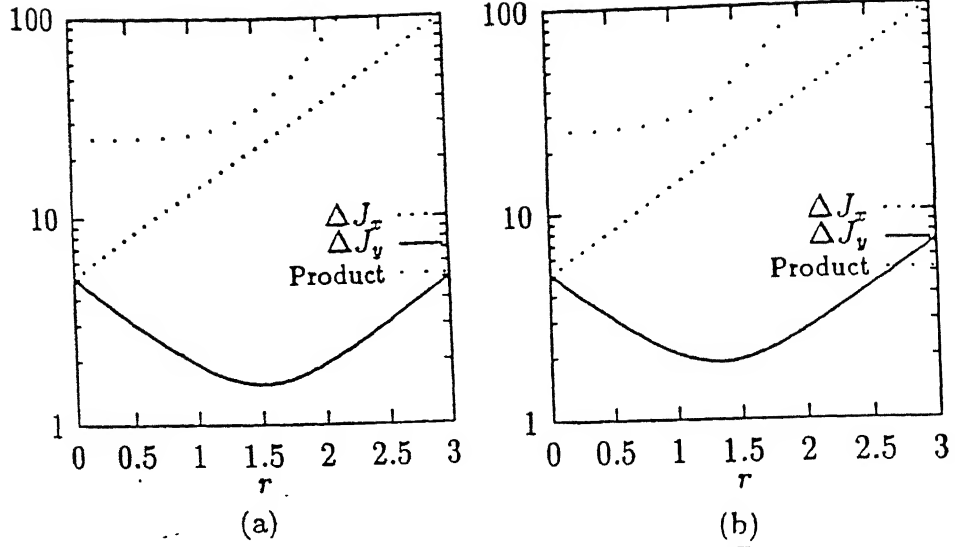


Figure 3.6: Comparison between single mode and double mode squeezing. (a) Variation of  $J_x$ ,  $J_y$  and their product with  $r$  for single mode squeezing with  $j = 50$ ,  $\delta = 0$  and  $m = -50$ , (b) Variation of  $J_x$ ,  $J_y$  and their product with  $r$  for double mode squeezing with  $j = 50$ ,  $m = -50$ ,  $\theta = 0$  and  $r_{\pm} = r$ .

angular momentum components for this special choice as

$$\begin{aligned} \Delta J_x^2 = & \frac{1}{2}[j + \sinh r_- \{\sinh r_- + \cosh r_- \cos(2\theta_+)\}(j + m) \\ & + \sinh r_+ \{\sinh r_+ + \cosh r_+ \cos(2\theta_-)\}(j - m) \\ & + \frac{\sinh^2 r_+ + \sinh^2 r_-}{2} + \sinh r_+ \sinh r_+ \cosh(r_+ + r_-)], \end{aligned} \quad (3.33)$$

$$\begin{aligned} \Delta J_y^2 = & \frac{1}{2}[j + \sinh r_- \{\sinh r_- - \cosh r_- \cos(2\theta_+)\}(j + m) \\ & + \sinh r_+ \{\sinh r_+ - \cosh r_+ \cos(2\theta_-)\}(j - m) \\ & + \frac{\sinh^2 r_+ + \sinh^2 r_-}{2} - \sinh r_+ \sinh r_+ \cosh(r_+ + r_-)], \end{aligned} \quad (3.34)$$

$$\begin{aligned} \Delta J_z^2 = & \frac{j + m}{4}[e^{2r_+} \cos^2 \theta_+ + e^{-2r_+} \sin^2 \theta_+] + \frac{j - m}{4}[e^{2r_-} \cos^2 \theta_- + e^{-2r_-} \sin^2 \theta_-] \\ & + \frac{1}{2}(\sinh^2 r_+ \cosh^2 r_+ + \sinh^2 r_- \cosh^2 r_-). \end{aligned} \quad (3.35)$$

The uncertainty ellipsoids are similar to that of single mode squeezing case. The uncertainties of the quadratures and their product are plotted in Fig 3.3.2 for

$r_+ = r_-$ ,  $j=50$ ,  $m=-50$ , and  $\theta_+ = \theta_- = 0$ . Here I have plotted the results for the extremum projection states which drops out the first term in both the quadrature uncertainties. The squeezing in the uncertainty of  $J_y$  prove our claim that double mode squeezing deteriorates the effect of single mode squeezing which was expected from qualitative reasoning. Squeezing both the modes by same amount retains the SU(2) symmetry of the system but the choice of the phases and magnitudes of coherent parameters breaks it resulting different expressions and curves for the quadratures. This choice has been made to show the difference distinctly and the dependence on the coherence phases. With all the parameters same for the two modes one can show that the two quadratures will behave similarly. Geometrical pictures for the double mode squeezing are similar to the single mode squeezing.

## Chapter 4

# Applications to two mode radiation system

Two mode radiation systems are of special interest in the field of optics due to interference related applications. This wave property reveals answers to the fundamental questions about quantum mechanics. Apart from the well known experiments in the under graduate courses, interferometers are used as very accurate measurement instruments to detect very feeble fluctuation caused by gravitational waves. Beam splitters (BS) is an essential component of an interferometer. It introduces a rotation in the angular momentum space. In this chapter I apply the several AM states to two mode systems.

In the first section a model of a lossy BS is developed. After representing the action of a BS as a scattering causing rotation in the AM space, I model the losses in medium due to the excitation of optical phonons. The losses were obtained in terms of the material properties. Using second order perturbation, the model yields Beer's law for absorption in the first approximation. Next I study the dissipative BS using SAMC and angular momentum eigen states. It will be shown that the fluctuations in the modes get increased because of the losses. The existence of quantum interference due to phase correlations between the input beams is observed. In spite of having such a dissipative medium, the result promises the possibility to design a lossless 50-50 BS at normal incidence which have potential applications in dielectric-coated

mirrors.

Next two sections deal with applications of SAMS states. Section two applies the SAMS states in a dual channel directional coupler. The coupled harmonic oscillator (CHO) hamiltonian of dual channel couplers introduces a time dependent rotation in the AM space. Using Pockel's effect coupling strength can be controlled externally. I have applied the SAMS states to study the transfer of quantum properties between the channels. The results show that the transferred squeezing to the initially coherent mode is of a new type. Application of SAMS states in increasing the accuracy of a Mach-Zehnder interferometer is discussed in the last section. It is shown that arbitrary increase in squeezing does not increase the accuracy of a interferometer. The estimate of the value of the amount of squeezing for the most accurate interferometric measurement is given.

## 4.1 Lossy BS

A beam-splitter (BS) is one of the most widely used optical component which is classically fully understood. However, as the use of non-classical sources of light in experiments increases[18, 14], it is essential to understand the behavior of all the components used in experiments in a purely quantum mechanical sense in order to interpret the results of these experiments as well as the limitations of these results. Several authors have considered the behavior of the lossless quantum mechanical BS[36, 37]. Unlike the classical case where merely the energy in one beam is split into two parts, a quantum-mechanical analysis shows that the BS modifies the basic statistical properties of the beams[37, 38]. Thus a simple BS can be used to probe the quantum nature of light by simple yet subtle experiments[39]. A BS offers one of the simplest interaction of a light mode with an external environment. It has been shown that damping of a mode due to interaction with a dissipative Gaussian reservoir can be approximated by a heuristic beam-splitter model[40]. In the first subsection I review the lossless quantum mechanical BS following the approach of

Prasad et al.[36].

Any real BS is also expected to have losses. In the next subsection, a model for the photon-phonon interaction and the consequent losses is developed. I choose to couple the radiation to the phonon-system because the lattice vibrations are accurately described by a harmonic oscillator model. Thus the light-matter interaction is easily modeled and yet most instructive. Most models of the interactions use advanced mathematical techniques. Here I have attempted to give a physical picture while keeping the mathematics as simple as possible. The model is true to a large extent in a host of dielectric materials in the microwave and the infra-red regions. Hence the model can be applied to a class of insulating materials with wide electronic bandgap. The analysis holds for low and moderate intensities of light with small losses so that the thermal equilibrium of the phonon reservoir is not disturbed. Even at zero temperature when there are no phonons present in the medium, the radiation field interacts with the vacuum states of the phonon system, undergoing losses and the fluctuations in the two modes get coupled. The spontaneous emission of light by the phonons comes out naturally in the model and this also contributes to the fluctuations though its contribution is lesser than that due to absorption.

In the next subsection the model is applied, in the first approximation for small losses, to a lossy medium to yield the classical Beer's law for absorption in a lossy medium. I develop a model for the losses in a medium due to the excitation of optical phonons in the medium. The medium is modeled to be a reservoir of phonons at some finite temperature and it is assumed that the photon-phonon interaction does not disturb the thermal equilibrium of the phonon system.

In the last subsection, the lossy BS is considered. Additional fluctuations, of greater order, are found due to the losses in the BS. Arguments are given how the total loss can be considered as a sum of losses in reflection, transmission and due to a quantum mechanical interference between the modes. The model prescribes the choice of the material properties of the BS to get the lossless case after considering the losses.

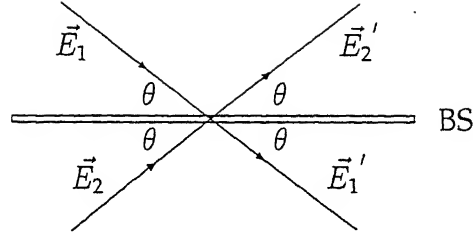


Figure 4.1: A beam-splitter with input and output light beams

#### 4.1.1 Representation of a BS in AM space

The general approach consists of breaking up the annihilation operators of the two interacting modes into two parts to correspond to the splitting of the beam in a manner that conserves the commutation relations. This causes the BS to couple the light modes. In Fig. 4.1, we show a lossless BS is shown with the two light waves  $\vec{E}_1$  and  $\vec{E}_2$  falling on from the two sides of it. Now both  $\vec{E}_1$  and  $\vec{E}_2$  give rise to the output waves  $\vec{E}_1'$  and  $\vec{E}_2'$ . Hence, for the positive components of the electromagnetic fields,

$$\begin{aligned} E_1^{(+)' } &= \alpha_{11} E_1^{(+)} + \alpha_{12} E_2^{(+)} , \\ E_2^{(+)' } &= \alpha_{21} E_1^{(+)} + \alpha_{22} E_2^{(+)} , \end{aligned} \quad (4.1)$$

where  $\alpha_{11}$  and  $\alpha_{21}$  are transmission and reflection coefficients for mode 1,  $\alpha_{12}$  and  $\alpha_{22}$  are reflection and transmission coefficients for mode 2. The coefficients could be dependent on direction ( $\vec{k}$ ) or polarization ( $\hat{e}_\lambda$ ) of the light mode. In the second quantized notation for the electromagnetic field, the  $E^{(+)}$  in the equations go over directly to the annihilation operators for the light modes. More conveniently in

matrix form one can write,

$$\begin{pmatrix} a_1' \\ a_2' \end{pmatrix} = \begin{pmatrix} \alpha_{11} & \alpha_{12} \\ \alpha_{21} & \alpha_{22} \end{pmatrix} \begin{pmatrix} a_1 \\ a_2 \end{pmatrix}. \quad (4.2)$$

Conservation of energy and preservation of the commutation relations between  $a_1'$  and  $a_2'$  leads to the relations

$$|\alpha_{11}|^2 + |\alpha_{21}|^2 = 1, \quad (4.3)$$

$$|\alpha_{12}|^2 + |\alpha_{22}|^2 = 1, \quad (4.4)$$

$$\alpha_{11} \alpha_{12}^* + \alpha_{21} \alpha_{22}^* = 0, \quad (4.5)$$

implying the transformation is unitary. Hence we look for a unitary operator  $\mathcal{U}$  such that,

$$\begin{pmatrix} a_1' \\ a_2' \end{pmatrix} = \mathcal{U}^\dagger \begin{pmatrix} a_1 \\ a_2 \end{pmatrix} \mathcal{U} = \begin{pmatrix} \alpha_{11} & \alpha_{12} \\ \alpha_{21} & \alpha_{22} \end{pmatrix} \begin{pmatrix} a_1 \\ a_2 \end{pmatrix}. \quad (4.6)$$

The operator  $\mathcal{U}$  turns out to be

$$\mathcal{U} = \exp[-i(\xi a_1^\dagger a_2 + \eta a_2^\dagger a_1)], \quad (4.7)$$

where  $\xi^* = \eta$  for  $\mathcal{U}$  to be unitary. Note that  $\mathcal{U}$  represents a rotation about  $J_x$  in the AM space. This relates the observable quantities  $\alpha_{ij}$  to the physical parameters  $\xi$  and  $\eta$  as,

$$\begin{pmatrix} \alpha_{11} & \alpha_{12} \\ \alpha_{21} & \alpha_{22} \end{pmatrix} = \begin{pmatrix} \cos \sqrt{\eta\xi} & -i\sqrt{\frac{\xi}{\eta}} \sin \sqrt{\eta\xi} \\ -i\sqrt{\frac{\eta}{\xi}} \sin \sqrt{\eta\xi} & \cos \sqrt{\eta\xi} \end{pmatrix}. \quad (4.8)$$

It is to be noticed that  $\alpha_{11} = \alpha_{22}$  and  $|\alpha_{12}| = |\alpha_{21}|$  i.e. the transmittance and reflectance are the same regardless of the wave vector  $\vec{k}$  with the crystal axis of the BS as the above relations were derived entirely from the boundary conditions and *de facto* assumed that the interaction due to the BS was isotropic and that the polarizations were not rotated either.



Choosing the photon state to be a product number state  $|n_1, n_2\rangle$ , where  $n_1$  and  $n_2$  are the number of photons in the light modes 1 and 2 respectively

$$\mathcal{U}|1, 0\rangle = \alpha_{11}|1, 0\rangle + \alpha_{21}|0, 1\rangle, \quad (4.9)$$

i.e., the final state is a coherent superposition of two single photon states in the two modes. The operation of  $\mathcal{U}$  on the  $|n_1, n_2\rangle$  state can be written as[36],

$$\mathcal{U}|n_1, n_2\rangle = \frac{1}{\sqrt{n_1!n_2!}}(\alpha_{11}a_1^\dagger + \alpha_{21}a_2^\dagger)^{n_1}(\alpha_{12}a_1^\dagger + \alpha_{22}a_2^\dagger)^{n_2}|0, 0\rangle. \quad (4.10)$$

The calculated fluctuations for pure number states  $|n_1, n_2\rangle$  and coherent states  $|\alpha, \beta\rangle$  are given by

$$\begin{aligned} \langle n_1, n_2 | (\Delta n_1)^2 | n_1, n_2 \rangle &= |\alpha_{11}|^2 |\alpha_{12}|^2 (n_1 + n_2 + 2n_1 n_2). \\ \langle \alpha, \beta | (\Delta n_1)^2 | \alpha, \beta \rangle &= (|\alpha_{11}|^2 + |\alpha_{12}|^2) |\alpha_{11}\alpha + \alpha_{12}\beta|^2. \end{aligned} \quad (4.11)$$

It is to be noticed that the coherent input modes are transformed into two completely uncorrelated coherent output beams by the action of the BS. This is due to the inherent SU(2) symmetry of the transformation[56].

#### 4.1.2 Radiation field-phonon interaction

Recognizing that the BS action occurs mainly due to lossless resonant scattering by orbital (bound) electrons in the atoms, the loss in the radiation field in the BS is modeled as due to the excitation of optical phonons in the BS i.e., the interaction of the photon field with the phonons in the BS. This causes energy to be irretrievably passed into the phonon energies. The BS is considered to be a reservoir of phonons at some finite temperature.

The phonon system is described by the phonon creation and annihilation operators  $b_k$  and  $b_k^\dagger$  defined as[57]

$$\begin{aligned} b_k &= \frac{1}{\sqrt{N}} \sum_{k=0}^{\infty} e^{i\vec{k}\cdot\vec{R}} \left[ \sqrt{\frac{M\omega_k}{2\hbar}} \vec{u}(\vec{R}) + i\sqrt{\frac{1}{2\hbar M\omega_k}} \vec{P}(\vec{R}) \right] \hat{e}_k, \\ b_k^\dagger &= \frac{1}{\sqrt{N}} \sum_{k=0}^{\infty} e^{-i\vec{k}\cdot\vec{R}} \left[ \sqrt{\frac{M\omega_k}{2\hbar}} \vec{u}(\vec{R}) - i\sqrt{\frac{1}{2\hbar M\omega_k}} \vec{P}(\vec{R}) \right] \hat{e}_k. \end{aligned} \quad (4.12)$$



Figure 4.2: Lattice displacements due to optical phonons : (a) transverse, (b) longitudinal.

satisfying the commutation relation  $[b_k, b_{k'}^\dagger] = \delta_{kk'}$  with the unperturbed Hamiltonian for the phonon reservoir as

$$R = \sum_{l=0}^{\infty} \hbar \omega_l (b_l^\dagger b_l + \frac{1}{2}). \quad (4.13)$$

$M$  is the mass,  $\vec{u}(\vec{R})$  is the displacement about the mean position,  $\vec{P}(\vec{R})$  is the momentum of the ion in the lattice;  $N$  is the total number of atoms in the crystal;  $\omega_k$  and  $\vec{k}$  are the frequency and the wave vector of the phonon. For simplicity only a single branch of the phonon modes are considered.

Classically the interaction energy of a charged particle with an electromagnetic field in the minimal substitution form is given by

$$V_i = \frac{q}{M} \vec{A}(\vec{R}) \cdot \vec{p} \quad (4.14)$$

We write the interaction energy for  $m$  charged ions in the lattice as  $V_I = m V_i$ . This can be done only for optical phonons. If the motion of the ions in the lattice due to optical phonons is observed, it looks as in Fig. 4.2. If any two adjacent ions are considered, the charges are opposite ( $q_1 = -q_2$ ) and their momenta are approximately equal in magnitude but opposite in direction ( $\vec{p}_1 = -\vec{p}_2$ ) and hence their energies add up. The positive and negative ions are assumed to be of approximately the same mass.

One has to exercise caution as the  $\vec{R}$  is a label for the second quantized electromagnetic field and also the position operator for the particle in the coordinate space.

Replacing  $\vec{A}(\vec{R})$  by the requisite operators in the Fock space,  $\vec{p}$  by the operator in the coordinate space, the compound operator acts on the states spanning the product space,

$$|\psi\rangle = \sum_j |j\rangle f_j(\vec{r}). \quad (4.15)$$

$\vec{A}$  acts on the  $|j\rangle$  states and  $p_\mu$  acts on the  $f_i(x^\mu)$ . Expressing  $\vec{A}$  in terms of the creation and annihilation operators of the electromagnetic field

$$\vec{A}(\hat{R}) = \sum_{k,\lambda} \sqrt{\frac{\hbar}{2\omega\epsilon V_{int}}} \left[ e^{i\vec{k}\cdot\hat{R}} a_{k\lambda} + e^{-i\vec{k}\cdot\hat{R}} a_{k\lambda}^\dagger \right] \hat{e}_\lambda, \quad (4.16)$$

where  $\hat{R}$  is the position operator for the particle and  $\vec{A}(\hat{R})$  means summation over the  $\vec{k}$  and nothing else.  $V_{int}$  is the volume of interaction of the beam inside the BS medium. It is to be noted that the role of  $e^{i\vec{k}\cdot\hat{R}}$  and  $e^{-i\vec{k}\cdot\hat{R}}$  are merely translations in the momentum space and preserve the conservation of momentum. Each time a photon of momentum  $\hbar\vec{k}$  is annihilated, the crystal momentum is increased by the same amount. Generally the photon momenta are small compared to the phonon momenta. In addition the BS splitter is kept clamped. Hence the conservation of momenta can be neglected to retain only the first term in the exponential i.e., unity.

The momentum  $\vec{p}$  of the particle can be expressed in terms of the  $b_k$  and  $b_k^\dagger$  operators,

$$\vec{p}(\vec{R}) = \sum_l i\sqrt{\frac{\hbar\omega_l M}{2N}} (b_l e^{-i\omega_l t} - b_l^\dagger e^{i\omega_l t}). \quad (4.17)$$

The interaction energy of the charged particle with the two modes of the electromagnetic field is

$$V_I = \sum_{i=1}^2 \sum_{l=0}^{\infty} \frac{iq\hbar m}{2} \sqrt{\frac{\omega_l}{\epsilon M V_{int} N \omega}} \left[ a_i b_l e^{-i(\omega+\omega_l)t} - a_i b_l^\dagger e^{-i(\omega-\omega_l)t} - a_i^\dagger b_l e^{i(\omega-\omega_l)t} + a_i^\dagger b_l^\dagger e^{i(\omega+\omega_l)t} \right]. \quad (4.18)$$

Now we seek the interaction averaged in time over several periods so that by the time interval the phonon reservoir has attained equilibrium. If this time is infinitely large, then on integration the exponentials yield,

$$\int_0^\infty e^{\pm i(\omega \pm \omega_l)t} dt = \pi \delta(\omega \pm \omega_l) \mp i\mathcal{P}\left(\frac{1}{\omega \pm \omega_l}\right), \quad (4.19)$$

where  $\mathcal{P}$  denotes the Cauchy principal value. Hence time averaged interaction

$$V_I = \sum_{i=1,2} \sum_l \hbar \kappa (\gamma_{il} a_i^\dagger b_l + \gamma_{il}^* a_i b_l^\dagger) G(\omega - \omega_l), \quad (4.20)$$

where, using  $m = \rho V_{int}$ ,

$$\gamma_{il} = (i\pi/2) q \sqrt{\rho V_{int} / \epsilon M V_x} \quad \hat{e}_{\lambda_i} \cdot \hat{e}_l. \quad (4.21)$$

where  $V_x$  is the crystal volume,  $\kappa$  is a constant of the order of unity and  $G(\omega - \omega_l)$  is a function sharply peaked at  $\omega = \omega_l$  depending on the observation time. As time tends to infinity,  $G$  tends to a  $\delta$ -function and  $\kappa$  becomes unity. The principal Cauchy value has been neglected as it is small. It's sole effect would have been to lead to a small shift in the frequency of the cavity mode.

The complete Hamiltonian of the radiation field and phonon system can be written down as

$$\mathcal{H}_T = \mathcal{H}_o + R + V_I, \quad (4.22)$$

where  $H_o = \hbar\omega(a_1^\dagger a_1 - a_2^\dagger a_2)$  is the free radiation hamiltonian,  $R$  is the free phonon Hamiltonian given in equation 4.11, and,  $V_I$  is the interaction term given by equation 4.16. If  $S$  is the density matrix for the coupled system, then the reduced density matrix given by taking the trace over the reservoir states

$$s = Tr_R[S] \quad (4.23)$$

and  $S_o = s_o f_o(R)$  before interaction of the photon and the phonon systems, where  $f_o(R)$  is the equilibrium distribution of the phonon states.

In the interaction picture the annihilation operators and the radiation states transform as

$$a'(t) = e^{i(\mathcal{H}_o + R)t/\hbar} a e^{-i(\mathcal{H}_o + R)t/\hbar}, \quad (4.24)$$

$$|\eta'\rangle = e^{-iV_I/\hbar} |\eta\rangle. \quad (4.25)$$

Due to the interaction of the radiation with the phonons the density matrix transforms as

$$S' = e^{iV_I/\hbar} S e^{-iV_I/\hbar}. \quad (4.26)$$

If the interaction between the photon and the phonon is not too strong it allows to consider terms only upto the second order in the expansion of the transformed density matrix

$$S' = S + i[V_I, S] - \frac{1}{2!}[V_I, [V_I, S]], \quad (4.27)$$

using the Baker Campbell Housdroff (BCH) relation

$$e^A B e^{-A} = B + [A, B] + \frac{1}{2!}[A, [A, B]] + \dots \quad (4.28)$$

Expanding the commutator and  $V_I$ , taking traces over the reservoir states to get the reduced density matrix, and using the cyclic property of traces and the ensemble averages,

$$\begin{aligned} \langle b_l \rangle_R &= \langle b_l^\dagger \rangle_R = 0, \\ \langle b_l b_k \rangle_R &= \langle b_l^\dagger b_k^\dagger \rangle_R = 0, \\ \langle b_l^\dagger b_k \rangle_R &= \bar{n}_{ph}(\omega_l) \delta_{lk}, \\ \langle b_l b_k^\dagger \rangle_R &= [\bar{n}_{ph}(\omega_l) + 1] \delta_{lk}, \end{aligned} \quad (4.29)$$

where  $\bar{n}_{ph}$  is the mean occupancy of the phonon levels which is nothing but the Bose-Einstein distribution  $\bar{n}_{ph}(\omega_l) = [\exp(\hbar\omega/kT) - 1]^{-1}$ , we get

$$\begin{aligned} s' = s &- (1/2) \sum_{i,j} (a_i^\dagger a_j s - a_i^\dagger s a_j - a_j s a_i^\dagger + s a_j a_i^\dagger) S_{ij} \\ &+ (a_i a_j^\dagger s - a_i s a_j^\dagger - a_j^\dagger s a_i + s a_j^\dagger a_i) S_{ij}^* \\ &+ (a_i^\dagger a_j s - a_j s a_i^\dagger) L_{ij} - (a_i s a_j^\dagger - s a_j^\dagger a_i) L_{ij}^*, \end{aligned} \quad (4.30)$$

where,  $L_{ij} = \sum_{l,k} \gamma_{il}(\omega_l) \gamma_{jk}^*(\omega_k) \langle \cos \theta_{il} \cos \theta_{jk} \rangle \delta(\omega - \omega_l) \delta(\omega - \omega_k) \delta_{lk}$  and averaging of  $\langle \cos \theta_{il} \cos \theta_{jk} \rangle$  is over a sphere. Markoff approximation has been used by implicitly assuming the interaction time scales much large than the correlation time of the phonon reservoir and much smaller than the cavity mode decay time, i.e.,  $\tau_{corr}^{(R)} \ll t_{int} \ll \tau_{decay}^{(s)}$ .

As  $\omega_l$  are closely spaced the summation over  $l$  goes over into an integral  $\sum_l \longrightarrow \int_0^\infty g(\omega_l) d\omega_l$ , where  $g(\omega_l)$  is the density of modes for the phonons, one

obtains the transformation of the reduced density matrix upto second-order, due to phonon interaction

$$L_{ij} = |\gamma(\omega)|^2 \langle \cos \theta_{il} \cos \theta_{jl} \rangle_{sphere} g(\omega), \quad S_{ij} = \bar{n}_{ph}(\omega) L_{ij}, \quad (4.31)$$

where  $\gamma = (i\pi/2)q\sqrt{\rho V_{int}/\epsilon M V_x}$ .

### 4.1.3 Lossy medium

The analysis of a simple transmission of a beam through the phonon medium using our formalism is instructive. The only interaction the light has with the medium is through the phonons. For a mixed state one has to calculate the trace over the photon states,  $\langle \hat{O} \rangle = \text{Tr} [s \hat{O}]$ . However, for a pure number state  $|n_1, n_2\rangle$  as the initial state, the density matrix is reduced to a single element  $s_o = |n_1, n_2\rangle \langle n_1, n_2|$ . The expectation values for the transformed beams for number states come out to be

$$\begin{aligned} \langle n_1, n_2 | a_1'^{\dagger} a_1' | n_1, n_2 \rangle &= n_1(1 - L_{11}) + S_{11}, \\ \langle n_1, n_2 | a_2'^{\dagger} a_2' | n_1, n_2 \rangle &= n_2(1 - L_{22}) + S_{22}. \end{aligned} \quad (4.32)$$

$L_{11}$  and  $L_{22}$  are the total absorption coefficients for the two modes. They represent the spontaneous emission (body-body radiation) by phonons in the two modes respectively. The coupling between the modes is not due to the phonon interaction. That is because such a process would correspond to a fourth order process (annihilation of a photon in one mode, creation of a phonon, annihilation of a phonon and creation of a photon in the other mode), and only upto the second order processes have been considered.

The fluctuations in the transmitted beam-1 is,

$$\langle n_1, n_2 | \Delta n_1^2 | n_1, n_2 \rangle = L_{11} (4 - L_{11}) n^2 + [2S_{11} + L_{11} (2S_{11} - 1)] n + S_{11} (1 - S_{11}). \quad (4.33)$$

It is noted that the absorption contributes in the coefficient of  $n^2$  while spontaneous emission appears only in the coefficient of  $n$ .

It is known that for small losses, Beer's law of absorption reduces to

$$\Delta I = I_0[1 - \exp(-\alpha l)] \approx I_0[1 - (1 - \alpha l)] = I_0 \alpha l, \quad (4.34)$$

where  $\alpha$  is the absorption coefficient per unit length. Considering the transmission of any one of the modes through a length  $l$ , the number of photons absorbed is

$$\delta n_1 = L_{11} n_1 = \left[ \frac{\pi^2}{12} \frac{q^2 \rho g(\omega)}{\epsilon M V_x} \right] A n_1 l, \quad (4.35)$$

i.e., it is proportional to the area of the beam and length traversed in the medium. If the density of modes for the phonons is considered as  $g(\omega) = \frac{\omega^2}{2\pi^2 v^3} V_x$ , then the present model predicts a dependence of absorption coefficient on frequency as  $\omega^2$ . The terms in the square bracket in equation 4.35 can be identified as the absorption coefficient.

#### 4.1.4 Lossy Beam-Splitter

When there is strong resonant scattering of light, then the  $a_i$  in the equation 4.30 go into  $a'_i$  according to equation 4.26. Taking the initial state to be pure number state,  $|n_1, n_2\rangle$ , we get

$$\begin{aligned} \langle n_1, n_2 | a'_1{}^\dagger a'_1 | n_1, n_2 \rangle &= (|\alpha_{11}|^2 n_1 + |\alpha_{12}|^2 n_2) (1 - L_{11}) \\ &\quad - \Re[L_{12}(\alpha_{11}^* \alpha_{21} n_1 + \alpha_{12}^* \alpha_{22} n_2)] + S_{11}. \end{aligned} \quad (4.36)$$

and a similar expression for  $\langle n_1, n_2 | a'_2{}^\dagger a'_2 | n_1, n_2 \rangle$ . Putting  $L_{11} = L_{22} = \frac{L}{2}$  and realizing  $L_{12} = \frac{L}{2} \sin \theta$ , the total loss reads

$$\mathcal{L} = \frac{L}{2} [(n_1 + n_2) - \sin |\xi| \sin \theta \sin 2\delta_\xi (n_1 - n_2)], \quad (4.37)$$

where  $\xi = |\xi| e^{i\delta_\xi}$ . The last equation shows that the interaction is purely dissipative, i.e., radiation field cannot gain energy from the medium. The cross-term, dependent on the incidence angle of the beams, is zero when the intensities are equal, and maximum when one of them is zero. This resembles the situation in scattering in a four-wave mixing process. When the intensity of one of the beams is zero one can

adjust the parameters of the second term can be adjusted to set the loss to zero. This happens only when  $\theta = \frac{\pi}{2}$ , i.e., it is a perfect 50-50 beam-splitter at normal incidence.  $\xi$  is dependent on the material properties. The no loss situation arises due to some kind of a quantum interference between the input beam and vacuum entering from the other port.

To get a further insight, the losses have been calculated for the initial coherent states  $|\alpha, \beta\rangle$ ,

$$\begin{aligned} \langle \alpha, \beta | a_1'^{\dagger} a_1' | \alpha, \beta \rangle &= |\alpha_{11}\alpha + \alpha_{12}\beta|^2 (1 - L_{11}) \\ &- \Re\{L_{12}(\alpha_{11}^* \alpha^* + \alpha_{12}^* \beta^*)(\alpha_{21}\alpha + \alpha_{22}\beta)\}. \end{aligned} \quad (4.38)$$

It is to be noticed that the two output beams do not go into completely uncorrelated coherent states. The losses break the inherent SU(2) symmetry of the BS transformation. The quantum interference terms in the losses reveal cross-correlation in the two modes. The total loss, taking into account both the beams, comes out to be

$$\begin{aligned} \mathcal{L} &= \frac{L}{2} [|\alpha|^2 + |\beta|^2 + 2|\alpha\beta| \sin\theta \{ \cos(\delta_\beta - \delta_\alpha) (\cos^2|\xi| - \sin^2|\xi| \cos 2\delta_\xi) \\ &+ \sin(\delta_\beta - \delta_\alpha) \sin^2|\xi| \sin 2\delta_\xi \}]. \end{aligned} \quad (4.39)$$

The loss can be written in the following form,

$$\mathcal{L} = \frac{L}{2} [|\alpha_{11}\alpha + \alpha_{12}\beta|^2 + |\alpha_{21}\alpha + \alpha_{22}\beta|^2 + 2 \sin\theta \Re\{(\alpha_{11}^* \alpha^* + \alpha_{12}^* \beta^*)(\alpha_{21}\alpha + \alpha_{22}\beta)\}]. \quad (4.40)$$

The above relation shows quantum correlation through interference terms. This is an observation new from the number state results. The difference in the behavior of the losses for the pure number states and the coherent states is thought to arise from phase correlation between the two input beams. In case of initial number states, the phase is completely random. The averaging of the  $\langle \cos \theta_{il} \cos \theta_{jl} \rangle_{sphere}$  in the interference term causes the average to go to zero for two equivalent number states incident upon two input ports. In the case of coherent input states two equal incident modes cause a constructive interference eliminating the losses. It has to be emphasised that these interference terms have a purely quantum origin and no



classical explanation is possible. Another evidence that this is a purely quantum phenomenon is that even when the beams are at grazing incidence this analysis gives a loss while any classical analysis would have yielded no losses. Calculating the fluctuations we find the absorption terms in the coefficients of the quadratic terms of the number of photons and spontaneous emission terms in the coefficients of the linear terms of the number of photons showing the effect of the losses on the photon statistics is greater than that of spontaneous emission.

## 4.2 Transfer of nonclassical properties in dual channel directional coupler

In the frame work of quantum optics devices employing control of light by another light could be well described by a simple model of two coupled harmonic oscillators[4]. A classical analysis of two coupled modes was given by Pierce[41]. He has shown that the two coupled modes exchange energies while propagating. The question naturally arises is that how do the non-classical properties are exchanged in the coupled harmonic oscillators during propagation. Will it be possible to transfer the non-classical properties from one mode to the other? This could have far reaching applications in experimental field where two modes could be chosen to be widely different in frequencies. If it is possible to transfer squeezing then in principle one could apply the scheme to generate squeezed light at higher frequencies which might not be feasible otherwise.

There have been several attempts to study this kind of coupled harmonic oscillator interactions. Love et al. studied the exchange of energy in beam propagation through a dual channel directional coupler[42]. As shown in fig. 4.3 , the coupler consists of a pair of optical waveguides which run in sufficiently close proximity, for a certain distance, so that coherent coupling takes place between them. When radiation passes through the structure, exchange of power between the channels is possible because of the evanescent field which is present in the region between

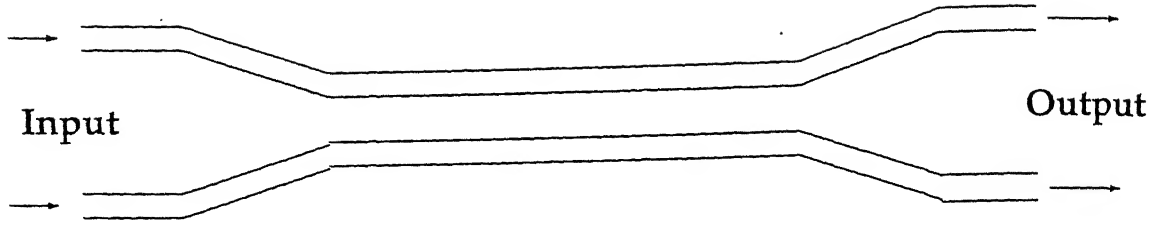


Figure 4.3: Dual Channel coupler with coupling controlled by Pockel's effect

them. The coupling characteristics is sensitively dependent upon the refractive index difference between the guides. In non-centrosymmetric nonlinear material, such as  $\text{LiNbO}_3$ , the refractive index can be controlled through the Pockel's effect. The coupling characteristics can thus be controlled by an external electrical signal which affects only the refractive index of the waveguide made up of such material. Lai et al. have discussed the photon statistics of non-classical fields in a linear directional coupler, where the losses can be negligible, using the number state as one of the inputs[43].

In the first subsection I describe the interaction and relate with a time dependent rotation in the AM space. Next subsection deals with the time development of the creation and annihilation operators. In this work we are interested in the transfer of the non-classical properties (squeezing, non-Poissonian statistics) from one mode to the other through the interaction (coupling) between two radiation fields. For this reason AM operators were not used. Next subsection discusses the results for the transfer of squeezing from one mode to the other. A new type of squeezing is observed in the induced mode. The last subsection presents the results of the time development of non-Poissonianness of the photon statistics in the induced mode.

### 4.2.1 Dual channel coupler as a time dependent continuous rotator

The Hamiltonian of the coupled harmonic oscillator is given by (in units of  $\hbar$ )

$$H = H_0 + V, \quad (4.41)$$

where  $H_0 = \omega_1 a_1^\dagger a_1 + \omega_2 a_2^\dagger a_2$  describes the free Hamiltonian and  $V = g(a_1^\dagger a_2 - a_2^\dagger a_1)$  is the interaction or coupling term under rotating wave approximation (RWA) with strength of the order of  $g$ . The interaction strength  $g$  can be calibrated and controlled by varying the electric field and thus the refractive index.  $\omega_i (= 2\pi\nu_i)$  are the measure of the frequencies  $\nu_i$ . Note that the interaction hamiltonian is similar to that of BS. The BS imparts a scattering effecting a rotation in the AM space, which depends on the reflectance and transmittance. In case of the dual channel coupler the rotation also depends on the time of interaction or the propagation length.

### 4.2.2 Time evolution of the operators

Choosing the central energy of the oscillators  $\hbar\omega_0$  ( $\omega_0 = \frac{\omega_1 + \omega_2}{2}$ ) to be zero and defining  $\delta = \frac{\omega_1 - \omega_2}{2}$ , the Hamiltonian reduces to

$$H = \delta(a_1^\dagger a_1 - a_2^\dagger a_2) + g(a_1^\dagger a_2 + a_2^\dagger a_1). \quad (4.42)$$

Solving the Heisenberg equation of motion for the creation and annihilation operators for the two modes and the above hamiltonian, their time evolution is found to be

$$\begin{bmatrix} a_1(t) \\ a_2(t) \end{bmatrix} = \begin{bmatrix} \mathcal{A}_1 & \mathcal{A}_2 \\ \mathcal{A}_2 & \mathcal{A}_1^* \end{bmatrix} \begin{bmatrix} a_1(0) \\ a_2(0) \end{bmatrix}, \quad (4.43)$$

and

$$\begin{bmatrix} a_1^\dagger(t) \\ a_2^\dagger(t) \end{bmatrix} = \begin{bmatrix} \mathcal{A}_1^* & -\mathcal{A}_2 \\ -\mathcal{A}_2 & \mathcal{A}_1 \end{bmatrix} \begin{bmatrix} a_1^\dagger(0) \\ a_2^\dagger(0) \end{bmatrix}. \quad (4.44)$$

where  $\mathcal{A}_1 = \cos \Omega t - i \frac{\delta}{\Omega} \sin \Omega t$ ,  $\mathcal{A}_2 = -i \frac{g}{\Omega} \sin \Omega t$ , with  $\Omega = \sqrt{\delta^2 + g^2}$ .

### 4.2.3 Transfer of squeezing

To calculate the different matrix elements of the observables showing nonclassical properties for the two modes we define our product oscillator state to be single mode SAMS state

$$|\Psi\rangle = |\psi_1\rangle \otimes |\psi_2\rangle = |\alpha_1, \xi\rangle \otimes |\alpha_2\rangle, \quad (4.45)$$

where the first oscillator is in squeezed coherent state  $|\alpha_1, \xi\rangle$  and the second one is in coherent state  $|\alpha_2\rangle$ .  $\alpha_i$  are complex coherence parameters of the two modes and  $\xi = re^{i\phi}$  is the squeezing parameter of the first mode. Using the results of time evolution of the creation and annihilation operators and setting  $\xi$  to be real and equal to be  $r$ , we calculate the uncertainties in the quadratures in the two modes (first index is for mode while the second index is for quadrature) for the state  $|\Psi\rangle$

$$\begin{aligned} \Delta X_{11}^2 &= \frac{1}{2} + |\mathcal{A}_1|^2 \sinh r [i \sinh r + \cosh r \cos 2\theta_{\mathcal{A}_1}], \\ \Delta X_{12}^2 &= \frac{1}{2} + |\mathcal{A}_1|^2 \sinh r [\sinh r - \cosh r \cos 2\theta_{\mathcal{A}_1}], \\ \Delta X_{21}^2 &= \frac{1}{2} + |\mathcal{A}_2|^2 \sinh r [\sinh r + \cosh r \cos 2\theta_{\mathcal{A}_2}], \\ \Delta X_{22}^2 &= \frac{1}{2} + |\mathcal{A}_2|^2 \sinh r [\sinh r - \cosh r \cos 2\theta_{\mathcal{A}_2}]. \end{aligned} \quad (4.46)$$

where,  $\theta_{\mathcal{A}_i}$  are the arguments of  $\mathcal{A}_i$  respectively. The terms in the square brackets can in general be negative according to the choice of parameters.

I have plotted their time evolution in figure(4.4) for  $|\alpha_1| = |\alpha_2| = 5.0$ ,  $g = \frac{\delta}{10}$  and  $\delta = 2 \times 10^{14}$ , which is in the visible range, with different  $r$  to show transfer of squeezing. Without interaction we would expect the uncertainties in quadratures of the first mode to oscillate sinusoidally with an argument of  $2t$ [58]. The figures 4.4(a-b) show sinusoidal oscillation, in the uncertainties of the quadratures with the argument  $\Omega t$ . This means that the amount of squeezing and period of oscillation of a squeezed beam can be controlled by another coherent beam. The control can be done through either the interaction strength i.e. the electric field or the frequency of the coherent beam. The plots in figs. 4.4(c-d) show that the squeezing is achieved in one quadrature of the second oscillator while the other quadrature is antisqueezed

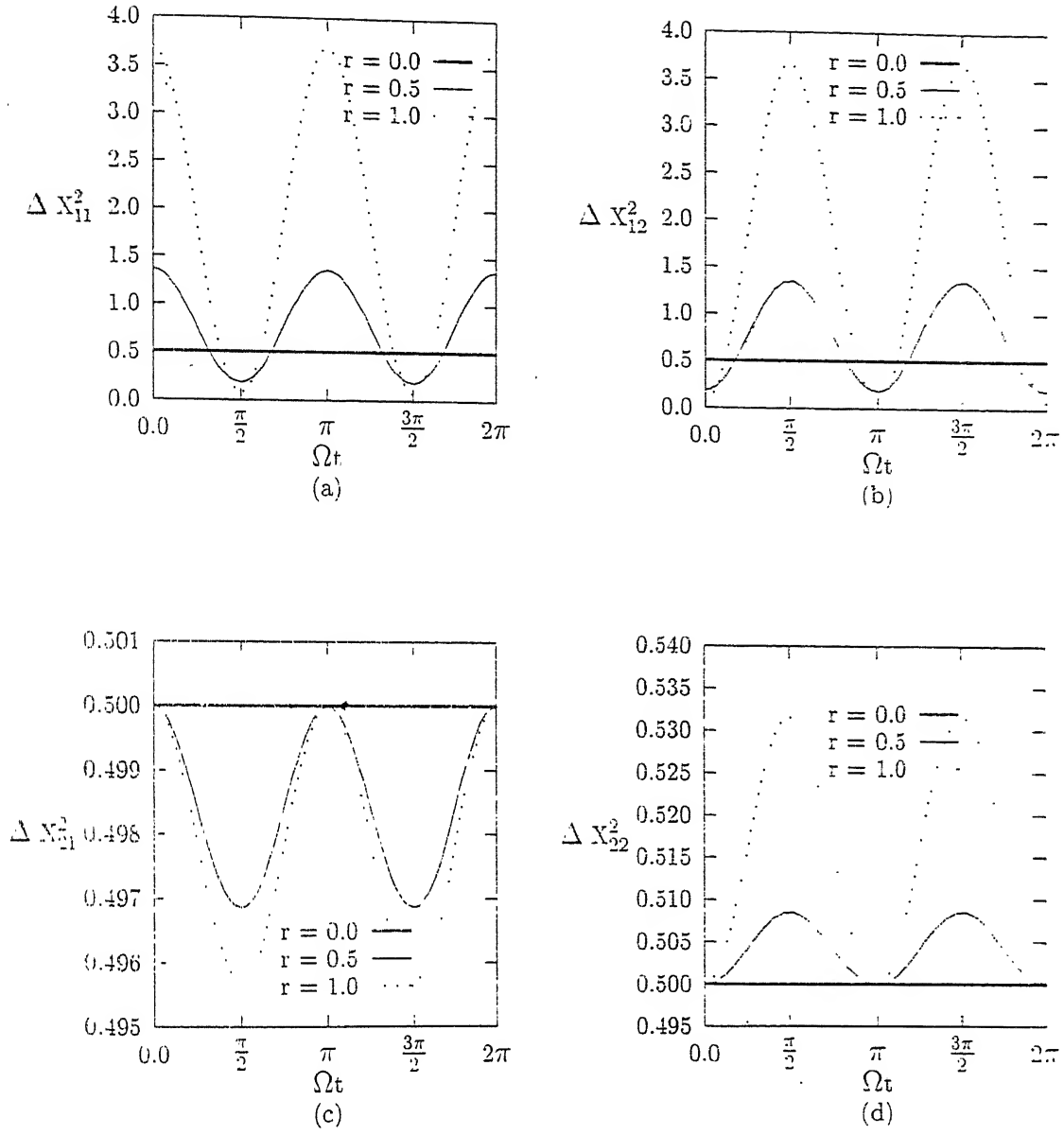


Figure 4.4: Variations of the quadrature uncertainties of both the modes with time for different  $r$ : (a) and (b) are the first and second quadratures of the first mode; (c) and (d) are the first and second quadratures of the second mode.

throughout the time. This is a new type of squeezing different from a squeezed beam generated by conventional processes. However, they oscillate in time with the same frequency  $\Omega t$  and come back to the coherent state periodically. In the case of single mode squeezing the uncertainty ellipse rotates in the phase space in time, but here the uncertainty circle deforms to ellipse and return back to circle in time. In the second cycle again the same quadrature is squeezed and the other quadrature antisqueezed. The amount of squeezing increases with the degree of squeezing of the first mode ( $r$ ) as expected. The squeezing can be reversed to the other quadrature of the second mode by simply setting  $\xi = -r$  ( $\phi = \pi$ ).

#### 4.2.4 Transfer of nonclassical number statistics

I have also calculated the mean and variances of the number operators for both the modes. The mean numbers are given by

$$\begin{aligned}\langle n_1 \rangle &= |\mathcal{A}_1 \nu|^2 + |\mathcal{A}_1 \alpha_1 + \mathcal{A}_2 \alpha_2|^2, \\ \langle n_2 \rangle &= |\mathcal{A}_2 \nu|^2 + |\mathcal{A}_2 \alpha_1 + \mathcal{A}_1 \alpha_2|^2.\end{aligned}\quad (4.47)$$

It is trivial to put the expressions of  $\mathcal{A}_i$  to observe that the mean numbers oscillate confirming the transfer of number of photons i.e. energy from one mode to the other. However, the total number operator  $\hat{N}$  ( $= \sum a_i^\dagger a_i$ ) remains invariant over time. Due to the interest about the statistics of the photon numbers in both the modes we have calculated the variances in the number as

$$\begin{aligned}\Delta n_1^2 &= [|\mathcal{A}_1 \nu|^2 + |\mathcal{A}_1 \alpha_1 + \mathcal{A}_2 \alpha_2|^2] + |\mathcal{A}_1|^2 \sinh r [\sinh r, \\ &\quad - 2|\mathcal{A}_1 \alpha_1 + \mathcal{A}_2 \alpha_2|^2 \{\sinh r - \cosh r \cos 2\theta_{\mathcal{A}_1 \alpha_1 + \mathcal{A}_2 \alpha_2}\}], \\ \Delta n_2^2 &= [|\mathcal{A}_2 \nu|^2 + |\mathcal{A}_2 \alpha_1 + \mathcal{A}_1 \alpha_2|^2] + |\mathcal{A}_2|^2 \sinh r [\sinh r, \\ &\quad - 2|\mathcal{A}_2 \alpha_1 + \mathcal{A}_1 \alpha_2|^2 \{\sinh r - \cosh r \cos 2\theta_{\mathcal{A}_2 \alpha_1 + \mathcal{A}_1 \alpha_2}\}].\end{aligned}\quad (4.48)$$

where,  $\theta_{\mathcal{A}_1 \alpha_1 + \mathcal{A}_2 \alpha_2}$  and  $\theta_{\mathcal{A}_2 \alpha_1 + \mathcal{A}_1 \alpha_2}$  are the phases of  $(\mathcal{A}_1 \alpha_1 + \mathcal{A}_2 \alpha_2)$  and  $(\mathcal{A}_2 \alpha_1 + \mathcal{A}_1 \alpha_2)$  respectively. Note that the number uncertainty of the first mode is no longer time-independent as in the case of a single squeezed radiation mode.

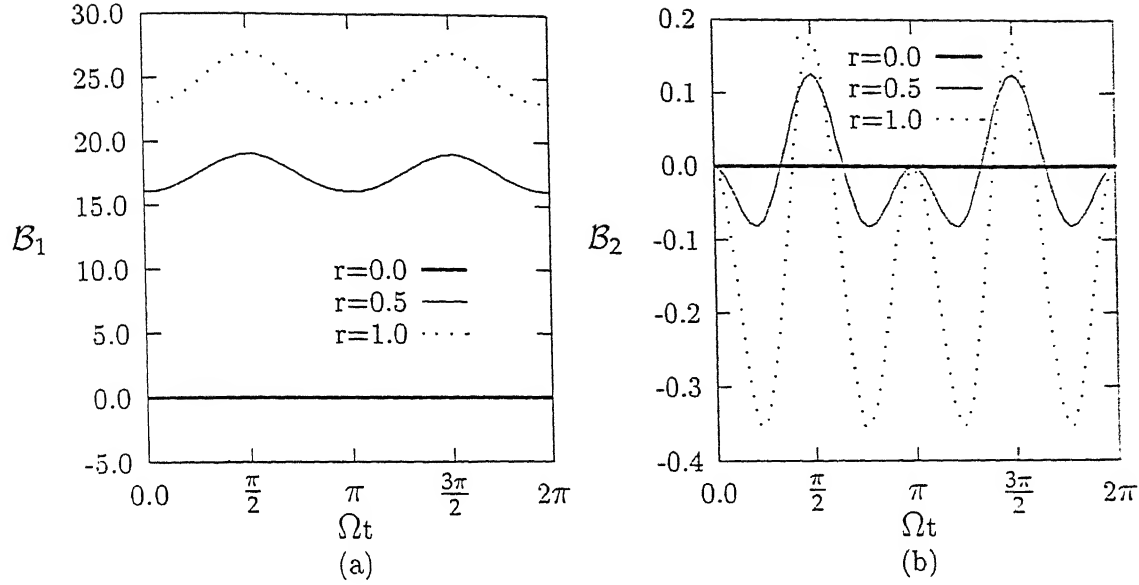


Figure 4.5: Variation of the statistical parameters of the (a) first mode and (b) second mode with time for different  $r$ .

The important features in the calculation of the number variables is not in the result of the mean or the uncertainties, but in the difference between them ( $B_i = \Delta n_i^2 - \langle n_i \rangle$ ), which is a measure of the statistics of the number of photons in the different modes. If  $B_i$  is positive or negative, then the statistics of that mode ( $i$ ) follows super- or sub-Poissonian statistics. In figure (4.5) I have plotted the time evolutions of  $B_i$ .  $B_1$  is no longer a constant difference between constant variance and constant mean[58], but oscillates in time. The oscillator was initially chosen to be super-Poissonian ( $B_1 > 0$ ) and the oscillation is small enough to maintain it to be super-Poissonian. But  $B_2$  shows both sub-Poissonian ( $B_2 < 0$ ) and super-Poissonian ( $B_2 > 0$ ) as it oscillates over time. The amount of sub-Poissonianness is seen to be more than super-Poissonianness for the second mode. Also the time spent with sub-Poissonian statistics is greater than the time spent as super-Poissonian.

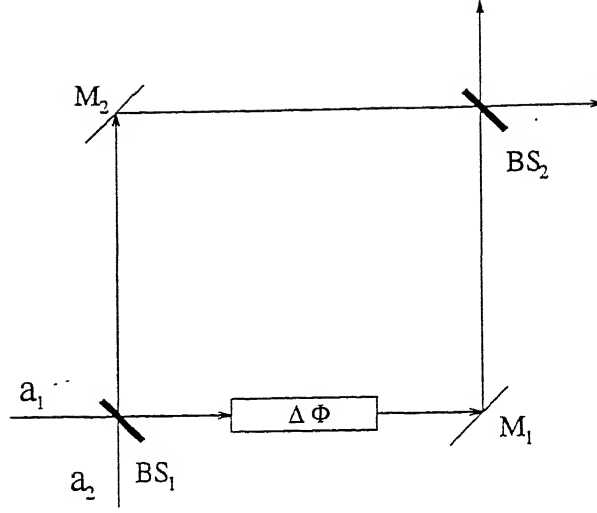


Figure 4.6: A typical Mach-Zehnder interferometer with two ports and a phase shifter.

### 4.3 Application to Interferometry

In this section I apply the single mode SAMS states to estimate the accuracy of an interferometer. First subsection describes an interferometer and defines the minimum detectable phase. In the next subsection the previous results are mentioned. Finally the current prescription and the results are discussed. An explicit estimation of the parameters for maximum accuracy is prescribed.

#### 4.3.1 Mach-Zender interferometer

An interferometer has typically two ports which can be perfectly described by the  $SU(2)$  group[20–22]. The accuracy of an interferometer is defined by the minimum detectable phase shift. The phase shift is generally determined by measuring the difference in the photon counting from the two output ports. Yurke *et.al.*[20] have defined the mean square noise or square of minimum detectable phase for Mach-



Zender interferometer (Fig. 4.6) as

$$\Delta\Phi^2 = \frac{\Delta J_z^2}{\left[\frac{d\langle J_z \rangle}{d\Phi}\right]^2} \quad (4.49)$$

Hillery and Mlodinow (HM)[21] have shown that the minimum detectable phase shift of the phase angle  $\Phi$  in a Mach-Zehnder interferometer can then be written as

$$\Delta\Phi = \frac{\Delta J_y}{|\langle J_x \rangle|} \quad (4.50)$$

### 4.3.2 Previous developments

If the input ports are coherent and vacuum respectively then the accuracy of the interferometer is  $\frac{1}{\sqrt{N}}$ , where  $N$  is the average of the mean number of photons in two ports[20, 21]. Yurke et al. achieved an accuracy of the order of  $\frac{2}{\sqrt{N}}$  using four wave mixers (FWM) where two modes are correlated as well as further squeezed. In HM's work, squeezed states, with certain choice of parameters, are chosen for the bosonic states. The squeezed states in both the modes are mixed (correlated) as well as introduced further squeezing by passing through a FWM again with certain choice of parameters. The states considered by them by the choice of parameters leads to an approximate estimation of the minimum detectable phase difference of  $\frac{e^{-2r}}{\sqrt{\langle N \rangle}}$ .

### 4.3.3 Present results

Current prescription uses Mach-Zehnder or any other interferometer consisting of only BS and no FWM. In the previous section it is shown that the action of the BS is to rotate the AM vector by a constant angle without introducing any further squeezing. This is in contrast to the previous work, where squeezing has been introduced through FWM while mixing the modes. In the current work the initial squeezing, in the oscillator quadratures, is utilized to squeeze out maximum squeezing for the phase measurement of the interferometer. It is shown in chapter 3

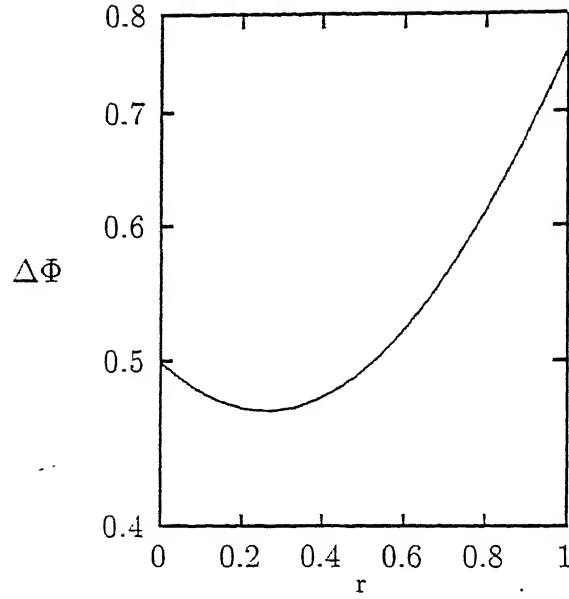


Figure 4.7: Variation of  $\Delta\Phi$  with  $r$  for  $n_+ = n_- = 16.0$  and  $\theta_+ = \theta_- = \frac{\phi}{2}$ .

that double mode squeezing worsens result, as far as squeezing in AM quadratures, increasing the minimum detectable phase difference.

One can simply rotate the single mode the SAMS states produced by optical nonlinear medium about  $J_x$  through an angle  $\frac{\pi}{2}$  by using beam splitter(s) of the interferometer. This changes the Z-axis to previous Y-axis retaining the X-axis towards the previous direction. Now, setting  $\delta = 0$  in equation 3.30 and combining with 3.29 and 4.50 in this rotated frame our new squeezed quadrature of phase angle becomes in terms of number operators

$$\Delta\Phi = \frac{\Delta J_y}{|\Re(\alpha_+ \alpha_-^*)|} = \frac{\sqrt{\frac{1}{16}[(1+n_-)e^{2r} + (1+3n_-)e^{-2r} + 2(2n_+ - 1)]}}{\sqrt{n_+ n_-} \cos(\theta_+ - \theta_-)} \quad (4.51)$$

From the last relation  $\Delta\Phi$  is plotted with  $r$  as the horizontal axis in Fig. 4.7 for  $\theta_+ = \theta_-$  and  $n_+ = n_- = \frac{N}{2} = 16.0$ . It is clear from the last relation that this choice of the phases of displacement and squeezing parameters leads to the minimum of  $\Delta\Phi$ . The choice of  $n_+$  and  $n_-$  are arbitrary. However, from the definition they must be positive real quantities. The numerical values of them indicate the intensities of the beams used in the interferometric measurement. The plot shows a minima

around  $r = 0.265$  which is a new feature. This observation tells that increase in the squeezing parameter does not guarantee monotonous decrease in  $\Delta\Phi$  throughout the range. The minimum can be calculated by differentiating the expression of  $\Delta J_y^2$  and equating it to zero as it is equivalent to  $\Delta\Phi$  minimum. We find the minimum in terms of number operator

$$r_{min} = \frac{1}{4} \ln \left[ \frac{1 + 3n_-}{1 + n_-} \right] \quad (4.52)$$

To achieve the maximum accuracy of the interferometer we simply take two (one coherent and the other squeezed) intense beams *i.e.* the expectation values of the number operators without squeezing ( $n_{\pm} = |\alpha_{\pm}|^2$ ) to be large enough. We rotate the angular momentum system as prescribed before in this section. The difference in the coherence parameter phases can be set to  $2n\pi$  and the phase of the squeezing parameter is made such to get  $\delta = 0$ . From the last relation and Fig 4.7 we get the desirable value of the squeezing parameter  $r$  for minimum detectable phase shift.

I have also calculated the phase uncertainty using the equation (3.4). The results show that the phase is not squeezed as it is. But the results described in this section show that a mere rotation can squeeze out the squeezing to the phase.

# Chapter 5

## Application in two level atomic system

In chapter 2 it is mentioned that a sample of ultra cold atoms in a certain level can be described as coherent states. SAMC states can represent an ensemble of ultra cold atoms in its ground state and one of the low lying excited states. In this chapter I study the interaction of coherent radiation with the two level ensemble of ultra-cold bosonic atoms. The level-spacing of the two levels is assumed to be resonant with the frequency of the coherent radiation. The calculations are done upto the approximation of second order in the perturbation theory. The results show generation of squeezing and other non-classical properties like photon antibunching of radiation. The interaction results to squeeze the dipole moment uncertainty of the atomic ensemble also. It is shown that with certain choice of the phases, amplification in the radiation is possible without inverting the average population difference .

### 5.1 Hamiltonian of the interaction

The interaction of small number of trapped two-level atoms are well studied[44]. The existing theory for the interaction of atoms with light waves adopted single particle density operator equation. The Hamiltonian of the combined atom field system in Jaynes-Cummings model[45] as (in units of  $\hbar$ )

$$H = H_A + H_F + V_I, \tag{5.1}$$

where,  $H_A = \omega_0 J_z$  is the Hamiltonian for the free two-level atom with energy difference of  $\omega_0$  between the levels,  $H_F = \omega a^\dagger a$  is the Hamiltonian of the free field with frequency  $\omega$ .  $V_I = g(aJ_+ + a^\dagger J_-)$  is the interaction term under rotating wave approximation (RWA) with interaction strength of  $g = \sqrt{\frac{6\pi^3 c^3 A}{V \omega^2}}$  [59].  $A$  is the  $A$ -coefficient of the two-level atoms in the mode volume  $V$ . For the resonance  $\omega$  becomes equal to  $\omega_0$ .

## 5.2 Time development of the operators

Due to the simplicity and resemblance with the classical perception I work in the Heisenberg picture, where any operator  $\hat{O}(0)$  is transformed to  $\hat{O}(t) = e^{iHt}\hat{O}(0)e^{-iHt}$  as time evolves. Using BCH relation 4.28 for operators and retaining the terms up to the second order for field operators and first order for angular momentum projection operator, it is possible to close the infinite series occurring in the transformed operators. The transformed linear operators of the field up to the order of  $g^2 t^2$  are

$$\begin{aligned} a(t) &= e^{-i\omega t}[a(0) - igtJ_-(0) - g^2 t^2 a(0)J_z(0)], \\ a^\dagger(t) &= e^{i\omega t}[a^\dagger(0) + igtJ_+(0) - g^2 t^2 a^\dagger(0)J_z(0)], \end{aligned} \quad (5.2)$$

and of the AM representing the atomic system up to the order of  $gt$  are

$$\begin{aligned} J_+(t) &= e^{i\omega t}[J_+(0) - 2igta^\dagger(0)J_z(0)], \\ J_-(t) &= e^{-i\omega t}[J_-(0) + 2igta(0)J_z(0)], \\ J_z(t) &= J_z(0) - igtaJ_z(0). \end{aligned} \quad (5.3)$$

Instead of calculating the transformation of the quadratic operators one can introduce the unity operator  $\exp(-iHt)\exp(iHt)$  between the linear operators. Thus simply multiplying the transformed linear operators one can find the product operators up to the order of the term in the transformed linear operators. These transformed product operators are used to calculate the different variances discussed below.

### 5.3 Initial state of the combined system

Now, we define the initial state of the whole system in the Schrodinger picture, i.e. the stationary state in the Heisenberg picture, as a product of the free field and the free atomic states  $|\Psi\rangle = |\psi_F\rangle \otimes |\phi_A\rangle$ . Choosing coherent radiation states for the field and SAMC states for the atoms we write

$$|\Psi\rangle = |\alpha\rangle \otimes |\beta_+, \beta_-\rangle. \quad (5.4)$$

where  $\alpha$  is the complex parameter of the coherent radiation field and  $\beta_i$  are the complex parameters for the angular-momentum coherent state.

### 5.4 Evolution of the field observables

Calculating the matrix elements of the time evolved operators for the above mentioned coherent-coherent states of the field and the atomic system we found the variances of the quadratures of the field variables up to the order of  $g^2 t^2$  as

$$\begin{aligned} \Delta X_1^2(t) = & \frac{1}{2} - 2gt|\alpha||\beta_+||\beta_-|[\sin(\theta_\alpha - \theta_{\beta_+} + \theta_{\beta_-}) + \sin(2\omega t - \theta_{\beta_+} + \theta_{\beta_-}) \\ & - 2\cos(\omega t - \theta_\alpha)\sin(\omega t - \theta_{\beta_+} + \theta_{\beta_-})] \\ & + g^2 t^2[|\beta_+|^2 + (|\beta_+|^2 - |\beta_-|^2)\{|\alpha|^2 \cos 2(\omega t - \theta_\alpha) - \frac{\alpha}{2} \cos(2\omega t - \theta_\alpha)\}], \\ \Delta X_2^2(t) = & \frac{1}{2} - 2gt|\alpha||\beta_+||\beta_-|[\sin(\theta_\alpha - \theta_{\beta_+} + \theta_{\beta_-}) - \sin(2\omega t - \theta_{\beta_+} + \theta_{\beta_-}) \\ & + 2\sin(\omega t - \theta_\alpha)\cos(\omega t - \theta_{\beta_+} + \theta_{\beta_-})] \\ & + g^2 t^2[|\beta_+|^2 - (|\beta_+|^2 - |\beta_-|^2)\{|\alpha|^2 \cos 2(\omega t - \theta_\alpha) - \frac{\alpha}{2} \cos(2\omega t - \theta_\alpha)\}], \quad (5.5) \end{aligned}$$

where  $\theta$ s are the phases or arguments of the complex parameters  $\alpha$  and  $\beta_\pm$ . For simplicity and a better understanding of the results we set all the phases ( $\theta$ s) to be zero, which does not reduce the importance of our results except that the linear dependencies on  $gt$  drops out.

As we are interested in the generation of non-classical properties, the second order term fulfills the purpose. Under this simplification the uncertainties reduce to

$$\Delta X_1^2(t) = \frac{1}{2} + g^2 t^2[|\beta_+|^2 + (|\beta_+|^2 - |\beta_-|^2)(|\alpha|^2 - \frac{|\alpha|}{2}) \cos 2\omega t],$$

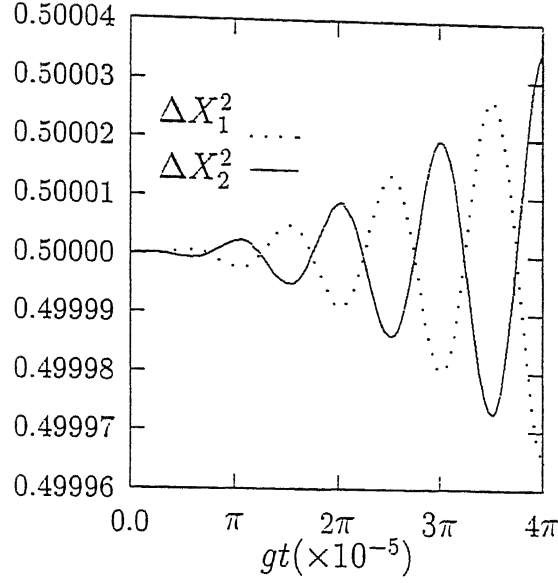


Figure 5.1: Variation of the uncertainties of the field quadratures with time

$$\Delta X_2^2(t) = \frac{1}{2} + g^2 t^2 [|\beta_+|^2 - (|\beta_+|^2 - |\beta_-|^2)(|\alpha|^2 - \frac{|\alpha|}{2} \cos 2\omega t)]. \quad (5.6)$$

I have plotted the time development of the uncertainties in Fig.5.1 for  $\nu = \frac{\omega}{2\pi} = 6 \times 10^{14} \text{Hz}$ ,  $g = \omega \times 10^{-5}$ ,  $|\alpha| = 5.0$ ,  $|\beta_+| = 1.0$ ,  $|\beta_-| = 10.0$ . The uncertainties in the quadratures show oscillations due to the sinusoidal term after a certain time and start to show squeezing properties. The amount of squeezing become more and more over time due to the  $(gt)^2$  dependency. However, the squeezing property also oscillates between the quadratures and at certain time intervals they return back to the coherent state.

I have also calculated the mean of the number of photons and statistics parameter  $B(= \langle a^{\dagger 2} a^2 \rangle - \langle a^\dagger a \rangle^2)$  for the above simplified choice of phases to check the amplification and non-classical behavior of the statistics of the photon number distribution. The mean number of the photons and  $B$  up to the order of  $g^2 t^2$  were calculated to be

$$\langle n(t) \rangle = |\alpha|^2 + g^2 t^2 [|\beta_+|^2 (1 + |\beta_-|^2) - |\alpha|^2 (|\beta_+|^2 - |\beta_-|^2)] \quad (5.7)$$

$$B = g^2 t^2 [|\beta_+|^2 (3 + |\beta_-|^2) - (|\alpha|^2 - |\alpha|)(|\beta_+|^2 - |\beta_-|^2)] \quad (5.8)$$

The expression of the mean number of photons has an extra term of the order of  $(gt)^2$

and thus if the quantity in the square bracket is chosen to be positive, amplification of the optical signal is possible through the interaction. The statistics parameter depends only on  $(gt)^2$  with a constant factor. If this constant factor, dependent only on the mean number of initial photons and the mean numbers of atoms in the two states, is chosen positive or negative, then it is possible to have non-Poissonian.

## 5.5 Evolution of the atomic observables

The angular momentum quadratures are actually the measure of the Bloch vector or the dipole moment of the atoms. We are interested in the position uncertainty of the Bloch vector in the AM space and the population inversion in the atomic system. I have similarly calculated the matrix elements for the atomic variables up to the order of  $gt$  but the results came out to be very much complicated in phase dependency and can not be understood directly. For this reason we present the results of the angular-momentum matrix elements of present interest, for the same choice of phases as in the last section,

$$\begin{aligned}\Delta J_x^2 &= \frac{1}{4}(|\beta_+|^2 + |\beta_-|^2) + 2gt|\alpha||\beta_+||\beta_-|(|\beta_+|^2 - |\beta_-|^2) \sin 2\omega t, \\ \Delta J_y^2 &= \frac{1}{4}(|\beta_+|^2 + |\beta_-|^2) - 2gt|\alpha||\beta_+||\beta_-|(|\beta_+|^2 - |\beta_-|^2) \sin 2\omega t, \\ \langle J_z \rangle &= \frac{1}{2}(|\beta_+|^2 - |\beta_-|^2)\end{aligned}\tag{5.9}$$

Unlike the case of the radiation, the linear dependencies of the quadratures of the atomic system on  $gt$  does not drop out for the simplified choice. However, the angular momentum projection or the population difference has linear dependency on  $gt$  which drops out for the choice of phases to be zero. The correction term present there for any phase is  $+2gt|\alpha||\beta_+||\beta_-| \sin(\theta_\alpha - \theta_{\beta_+} + \theta_{\beta_-})$ . If the phases are chosen to make this term non-zero, then population difference can also be controlled through the interaction. This means that the population inversion can also be controlled by the choice of the phases. However, as we are interested in optical amplification, it is shown that the simplified choice of the phases can amplify the optical signal even



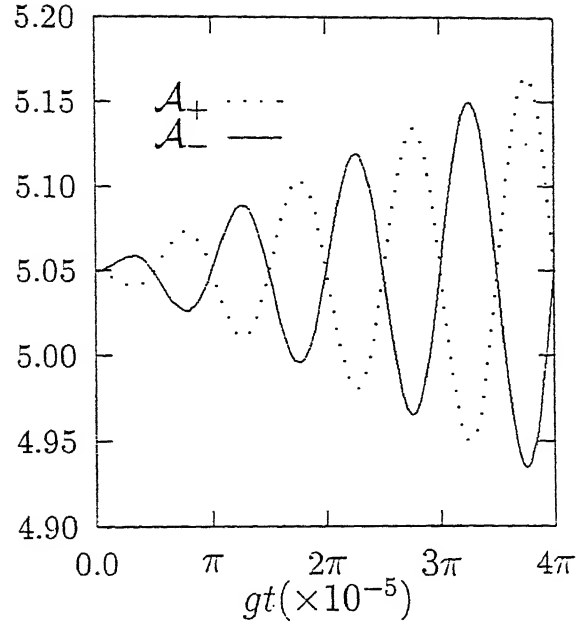


Figure 5.2: Variation of the uncertainties of the normalized atomic quadratures with time.

without any effective population inversion in the ensemble of two condensates.

I have the normalized quadratures  $\mathcal{A}_+ = \frac{\Delta J_z^2}{|(J_z)|}$  and  $\mathcal{A}_- = \frac{\Delta J_z^2}{|J_z|}$  are plotted in fig 5.5 for the same choice of parameters as in the case of field. The uncertainty of the AM quadratures are clearly seen to go below its coherent state value, showing signature of atomic or AM squeezing. Though the plot promises to show greater squeezing after long time interval, but the present calculation breaks down at the regime without ensuring the nature of the plot. It is noticed that the uncertainties oscillate in time with opposite phase and come back to the initial value with a periodicity like the field case. One more difference in the plots is that the field starts showing the interaction effect only after some time whereas the atoms are affected as soon the interaction starts. Also notice that we have not started from the minimum uncertainty (though coherent by definition) angular-momentum states where all the atoms are coherently either in ground ( $|\beta_+| = 0$ ) or in excited state ( $|\beta_-| = 0$ ) as this will drop all effects on the quadratures of the atomic system and the it will remain at minimum uncertainty state throughout.

# Chapter 6

## Conclusions

In this thesis, I have studied the angular momentum coherent and squeezed states with some quantum optical applications. I have studied the two definitions of angular momentum coherent states, with the physical systems represented by the definitions. It is found that one of the definitions (SAMC states) qualify as a better candidate for AM coherent states than the other one (CSS). CSS are rotated angular momentum ground states. The projections of these rotated states in X-Y plane is an ellipse and thus show squeezing. Physically, mere rotation should not change the status of the state. This question has been raised by Kitagawa and Ueda[29] that if CSSs describe squeezed angular momentum states under suitable choice of coordinates. The definitions are compared geometrically.

Following the similar procedure to construct SAMC states I have constructed the angular momentum squeezed (SAMS) states and studied their properties for a simple choice of parameters. These simplifications does not hamper the qualitative geometrical interpretation of these states. Actually, consideration of all the parameters makes the results complicated and not easily visible in the phase space picture. Due to this reason we have simplified the results by these choices. It is shown from numerical plots that they really squeeze angular momentum operators. The SAMS states are geometrically represented to show the ellipsoidal nature of the uncertainties. It is also shown that two mode squeezing deteriorates the squeezing effect in

angular momentum quadratures.

The geometrical representation presents a better understanding of the structure and the dynamics of the states. Feynman *et al.* [24] have shown that the components of the pseudo angular-momentum vector completely specifies the state of the system semiclassically. In this thesis I have discussed the quantum uncertainties, not discussed by them. The power of the geometrical method developed by Feynman *et al.*, lies in visualizing and solving problems involving transition between two quantum levels. Geometrical methods are found useful for problems that can be solved analytically. It can also provide valuable insight into the behavior of the processes that are insolvable by analytical technique. In the definition of SAMC and SAMS states the difficulty in representation is overcome and the question of Kitagawa is answered. The geometrical picture developed in this thesis for SAMC or SAMS states does not have ambiguity and thus is a better representation for the angular momentum coherent and squeezed states.

The coherent and squeezed AM states were used for two mode radiation system in the fourth chapter. I have modeled a lossy beam splitter with the losses being due to the excitation of optical phonons in the medium. The model yields an expression for the absorption coefficients in terms of the material properties of the BS. It is assumed the losses due to electron conduction negligible. Hence the model applies to a class of insulating materials with wide electronic bandgap. The analysis holds for low and moderate intensities of light with small losses so that the thermal equilibrium of the phonon reservoir is not disturbed. Even at zero temperature when there are no phonons present in the medium, the radiation field interacts with the vacuum states of the phonon system, undergoing losses and the fluctuations in the two modes get coupled. It is shown how fluctuations increase as compared to the lossless case. Also the spontaneous emission of light by the phonons comes out naturally in the model and this also contributes to the fluctuations though its contribution is lesser than that due to absorption. The model prescribes the choice of the material properties of the BS to get the lossless case after considering the losses. It is argued how the

total loss can be considered as a sum of losses in reflection, transmission and due to a quantum mechanical interference between the modes.

For the next application, I have calculated the uncertainties in the quadratures and the bunching parameter for both the modes as a function of time to show that the sharing of the non-classical properties of a squeezed harmonic oscillator to a coherent (classical) one is possible when they are coupled. The procedure is supported by an experimental scheme of dual channel directional coupler for coupling between two light modes propagating in the two waveguides. The experimental situation can also be achieved where two quantum radiations of different frequencies interact through a medium consisting of three-level atoms. The energy difference of the allowed transitions of the atom should be resonant to that of the radiations or vice versa. The interaction effect generated by the atoms has to be described totally by the interaction strength  $g$ . However, in the three-level atomic system and two-mode light interaction involves the atomic SU(3) operators in the interaction hamiltonian. This interaction is greatly simplified in the present hamiltonian by expressing the atomic operator effect by the interaction strength  $g$ , a number. In the simplified approach, the system can be described by the coupling hamiltonian. As pointed out by Lai et al.[43] the coupling of the lossless directional coupler is of course related to the lossless beam splitter (BS) in the way both of the procedures couple the two quantized field modes. In the case of the directional coupler it is possible to study the time development (or the development of the observables over the propagation distance), whereas in the case of thin BS it is treated as a scattering matrix. However, the case of a thick BS, where the coupling occurs over a certain thickness (or for a certain time interval), is exactly the case of the present discussion. The transfer of squeezing clearly depends on the interaction strength or in other words on the ratio of it with the frequency difference between the oscillators. The squeezing generated in the second mode is shown to be different in nature than single mode squeezing which is a totally new phenomenon. It is also shown that the photon statistics of the affected mode can be made sub- or super-Poissonian. The procedure given here

could help in controlling nonclassical states of radiation and generating a new kind of squeezed states for applications in quantum optics.

I have applied the SAMS states in analyzing the sensitivity of SU(2) interferometers. The effect of two mode squeezing on interferometry can be seen from the results of the uncertainties in two mode squeezing. As two mode squeezing increases the uncertainty of the squeezed quadrature it will also increase the value of minimum detectable phase difference ( $\Delta\Phi$ ) of any interferometer using beam splitters. The relation between them in the frame rotated by  $\frac{\pi}{2}$  about X axis can be written as  $\Delta\Phi = \frac{\Delta J_y}{|J_x|}$  [22]. Application of our results for the SAMS states reveal the fact that they can reduce the minimum detectable phase, thereby increasing the accuracy of the interferometer. The parametric values for the maximum accuracy are estimated. Gravitational waves produce very small  $\Delta\Phi$  which can hopefully be detected following our prescription without using FWM. Fermion interferometry can be considered by changing the bosonic commutation relation to the anticommutation relation for fermions. This is a totally new possibility as no fermion analog of the boson squeezed states has yet been found [60].

A two level atom can be considered as a spin- $\frac{1}{2}$  particle. However, they do not have to follow the Pauli exclusion principle for fermions. A collection of these atoms can be described by the SU(2) algebra of angular momentum systems [27, 26]. In fact the complete set to describe the system is achieved by adding a permutation group  $P_N$  to the SO(3) group which does not change the basic essence of the formalism. The number operators ( $\hat{n}_{\pm} = j \pm m$ ) in the case of interferometry represent the population or occupation numbers in the upper and lower states the atomic system.

Recent experiments [8–11] to produce ultra cold atomic samples reveal that at such low temperatures and high densities the de Broglie wavelength of an atom becomes comparable to the sample size. For such samples, the effect of quantum statistics becomes crucially important [12], and are expected to have properties similar to the role of lasers in conventional coherent optics [13]. This property allows one to express a condensate by simplistic representation of coherent state of a harmonic oscillator.

If there are two such samples at two different levels, the combined system can be described by SAMC state.

I have studied the change in the field and atomic variables in the interaction of coherent radiation and ultra-cold two-level atomic ensemble, represented by the simplistic model of SAMC states, using the rotating wave approximation (RWA) in Jaynes-Cummings Model for the Hamiltonian retaining the terms of the order of square of the interaction strength for the field variables and the terms of the order of the interaction strength for the atomic variables. We show that under these approximations the interaction produces squeezing in the initially coherent radiation field. It is shown that the statistics of the photon number of the radiation field can be made non-Poissonian through the interaction. We have calculated the effect of the interaction on the atomic system in coherent angular-momentum state and prescribed a method to reduce the uncertainties in the atomic quadrature in expense of the other. From the numerical plots it is seen that the interaction produces atomic squeezing. There was proposal of certain inter-atomic interaction for generation of angular momentum squeezing[29]. However, no practical experimental scheme was proposed to generate them. The current scheme promises to generate squeezing in atomic or pseudo-angular momentum systems. Amplification in the radiation field without any population inversion in the atomic system is found. It is observed that the uncertainties of the atomic system show similar oscillatory dependence over time.

The angle quadrature corresponding to the angular momentum needs some physical understanding in the context of two dimensional harmonic oscillators. Nieto[48] developed a procedure to treat the oscillators in  $\pm$  basis as created from two oscillators quantized in the X and Y directions. To follow his prescription, we have to express the squeezing operator in X-Y basis. This creates some disentanglement problem. The problem can be handled by putting certain constraints on the parameters. It does not arise in the case of SAMC states. The connection between SAMC states and coherent states of two dimensional oscillator is trivial[28], which is not so

for SAMS states.

$Sp(4, \mathbb{R})$  group, describing all two mode quadratic transformations, can be divided into two classes : (i) the *passive*  $U(2)$  subgroup, which does not change the degree of squeezing, and, (ii) the *active* elements, which impart squeezing into the system[32]. The active group contains six elements. The  $SU(2)$  or AM is a subgroup of  $U(2)$ . It will be interesting to connect the uncertainties in both the representations. While describing the interaction between two mode radiation system and a three level atomic system. The  $SU(3)$  operators, describing the atomic system, may or may not introduce squeezing. In case of BS, with three level material, this effect can affect the simple BS effect, a pure rotation. The study of the combined system can reveal interesting physics.

# Appendix A

To calculate the expectation values and variances of  $J_x$ ,  $J_y$  and  $J_z$  we write these operators in terms of bosonic operators as

$$\begin{aligned} J_x &= \frac{1}{2}(a_+^\dagger a_- + a_+ a_-^\dagger), \\ J_y &= \frac{1}{2i}(a_+^\dagger a_- - a_+ a_-^\dagger), \\ J_z &= \frac{1}{2}(a_+^\dagger a_+ - a_-^\dagger a_-). \end{aligned} \quad (\text{A.1})$$

and their squares in terms of number operators and ladder operators of angular momentum

$$\begin{aligned} J_x^2 &= \frac{1}{4}[J_+^2 + J_-^2 + 2(J_+ J_- - J_z)], \\ J_y^2 &= -\frac{1}{4}[J_+^2 + J_-^2 - 2(J_+ J_- - J_z)], \\ J_z^2 &= \frac{1}{4}[\hat{n}_+^2 + \hat{n}_-^2 - 2\hat{n}_+ \hat{n}_-]. \end{aligned} \quad (\text{A.2})$$

where  $\hat{n}_\pm = a_\pm^\dagger a_\pm$  and  $J_\pm$  are defined in subsection (3.2.2). Now, we define a new set of primed operators after operating the necessary displacement ( $\tilde{D} = D_+ D_-$ ) and squeezing ( $S$ ) operators as needed due to our definition of single mode SAMS states act on it,

$$X' = S^{-1}(\xi) D_+^{-1}(\alpha_+) D_-^{-1}(\alpha_-) X D_-(\alpha_+) D_+(\alpha_-) S(\xi) \quad (\text{A.3})$$

Notice that the operators in the separate modes ( $\pm$ ) commute with each other as they are defined to be uncorrelated. So, one can separately operate them on the two



sets ( $\pm$ ) of normally ordered bosonic operators occurring in the angular momentum operators ( $J_{\pm}$  and  $J_z$ ) and their squares and product ( $J_+ J_-$ ) operators. One has to take care that any operator  $X$ , expressed in terms of bosonic operators, is always normally ordered ( $:X:$ ) after any set of  $A^{-1} : X : A$  operation. Then taking their expectation values about the ground state  $|0, 0\rangle$ , we get

$$\begin{aligned}
\langle J_+ \rangle &= \alpha_+^* \alpha_-, \\
\langle J_- \rangle &= \alpha_-^* \alpha_+, \\
\langle J_z \rangle &= \frac{1}{2}(|\alpha_+|^2 - |\alpha_-|^2 + \sinh^2 r), \\
\langle J_+^2 \rangle &= (\sinh r \cosh r e^{-i\phi} + \alpha_+^{*2} \alpha_-^2), \\
\langle J_-^2 \rangle &= (\sinh r \cosh r e^{i\phi} + \alpha_-^2 \alpha_+^{*2}), \\
\langle J_z^2 \rangle &= \frac{1}{4}[|\alpha_+|^4 + |\alpha_-|^4 + |\alpha_+|^2 \{1 + 2 \sinh r [2 \sinh r - \cosh r \cos(\phi - 2\theta_-)]\} \\
&\quad + |\alpha_-|^2 \{1 - 2(|\alpha_+|^2 + \sinh^2 r)\}], \\
\langle J_+ J_- \rangle &= (|\alpha_+|^2 + \sinh^2 r)(|\alpha_-|^2 + 1).
\end{aligned} \tag{A.4}$$

Putting the results of A.4 in A.1 and A.2 and recollecting the definition of variance,  $\Delta X^2 = \langle \psi | X^2 | \psi \rangle - \langle \psi | X | \psi \rangle^2$  we get the mean and variances of  $J_i$  in terms of the variables  $\alpha_{\pm}$ . Using the definitions :  $\alpha_{\pm} = \sqrt{n_{\pm}} e^{i\theta_{\pm}}$ ,  $j = \frac{1}{2}(n_+ + n_-)$  and  $m = \frac{1}{2}(n_+ - n_-)$ , we can express them as

$$\begin{aligned}
\langle J_x \rangle &= \Re(\alpha_+ \alpha_-^*), \\
\langle J_y \rangle &= \Im(\alpha_+ \alpha_-^*), \\
\langle J_z \rangle &= m + \frac{1}{2} \sinh^2 r,
\end{aligned} \tag{A.5}$$

$$\begin{aligned}
\Delta J_x^2 &= \frac{1}{2}j + \frac{1}{2} \sinh r \left[ \frac{1}{2} \sinh r \{1 + 2(j - m)\} + (j - m) \cosh r \cos \delta \right], \\
\Delta J_y^2 &= \frac{1}{2}j + \frac{1}{2} \sinh r \left[ \frac{1}{2} \sinh r \{1 + 2(j - m)\} - (j - m) \cosh r \cos \delta \right], \\
\Delta J_z^2 &= \frac{1}{4} \Delta N^2 = \frac{1}{4} \Delta n_+^2 + \frac{1}{4} \Delta n_-^2 \\
&= \frac{1}{4} |\alpha_+|^2 [e^{2r} \cos^2 \eta + e^{-2r} \sin^2 \eta] + \frac{1}{2} \sinh^2 r \cosh^2 r + \frac{1}{4} |\alpha_-|^2.
\end{aligned} \tag{A.6}$$

with  $\delta = 2\theta_- - \phi$  and  $\eta = \theta_+ - \frac{\phi}{2}$ . The observations on the number uncertainty appearing in the last equation is discussed with phase by Loudon[18] in the context of boson squeezing.

# Bibliography

- [1] E. C. G. Sudarshan, Phys. Rev. Lett. **10**, 277 (1963)..
- [2] R. J. Glauber, Phys. Rev. **130**, 2529 (1963); Phys. Rev. **131**, 2766 (1963); Phys. Rev. Lett. **10**, 84 (1963).
- [3] J. R. Klauder, Journ. Math. Phys. **4**, 1055 (1963); *ibid.*, 1058 (1963).
- [4] W. H. Louisell, in *Quantum Statistical Properties of Radiation* Wiley Interscience, (1973); J.R. Klauder and E. C. C. Sudarshan , in *Fundamentals of quantum optics*, W. A. Benjamin, NY (1968); L.Mandel and E. Wolf, in *Coherence and quantum optics*, Cambridge, NY (1995).
- [5] E. Schrödinger, Naturwissenschaften **14**, 664 (1926).
- [6] *Coherent States*, ed. J. R. Klauder and B. S. Skagerstam, World Scientific ,Singapore, 1985.
- [7] M.M.Nieto and D.R.Traux, Phys.Rev. Lett. **71**, 2843 (1993).
- [8] C. Monroe, W. Swann, H Robinson and C. Wieman, Phys. Rev. Lett. **65**, 1571(1990); J.M.Doyle, J.C.Sandberg, I.A.Yu, C.L.Cesar, D.Kleppner and T.J.Greytak, Phys. Rev. Lett. **67**, 603 (1991).
- [9] M. H. Anderson et al., Science **269**, 198 (1995).
- [10] C.C.Bradley, C.A.Sackett, J.J.Tollett and R.G.Hulet, Phys. Rev. Lett. **75**, 1687 (1995).

- [11] K.B.Davis, M.-O. Mewes, M.R.Andrews, N.J. van Druten, D.S.Durfee, D.M.Kurn and W.Ketterle, Phys. Rev. Lett. **75**, 3969 (1995).
- [12] K. Burnett, Contemporary Physics **37**, 1 (1996).
- [13] W. Zhang and D. F. Walls, Phys. Rev. A **49**, 3799 (1994); Phys. Rev. Lett. **76**, 161 (1996).
- [14] D. F. Walls and G. J. Milburn in *Quantum Optics*, Springer Verlag(1994).
- [15] H. P. Yuen, Phy. Lett. **51 A**, 1 (1975); Phys. Rev. A **13**, 2226 (1976).
- [16] M. C. Teich and B. A. E. Saleh, Quantum Optics,**1**, 151 (1989).
- [17] D. R. Traux, Phys. Rev. D **31**, 1988 (1986); M. M. Nieto, in *Frontiers of Non-equilibrium Statistical Mechanics*, Proceedings of NATO Advanced Study Institute, ed. G. T. Moore and M. O. Scully, Plenum, NY.
- [18] D. F. Walls, Nature, **306**(1983)141; R.W.Henry and S.C.Glotzer, Am. J. Phys.**56**, 318 (1988); R. Muñoz-Tapia, Am. J. Phys.**61**, 1005 (1993); R.Loudon, Journ. of Mod. Optics**34**, 709 (1987); J. H. Shapiro, IEEE, J. Quant. Electron. **QE-21**, 237 (1985); C. M. Caves, in *Coherence, cooperation, and fluctuations*, ed. F. Hakke, L. M. Narducchi and D. F. Walls, Cambridge (1985); R. E. Slusher and B. Yurke, Sci. Am. **258**, 50 (1988). See also the special issues devoted to squeezed states as J. Mod. Opt. **34** (1987) and J. Opt. Soc. Am. **b 4**, (1987).
- [19] D. Stoler, Phys. Rev. D **1**, 3217 (1970); Phys. Rev. bf D **4**, 1925 (1971); C. Caves, Phys. Rev. D **23**, 1693 (1981).
- [20] B. Yurke, S. L. McCall, J. R. Klauder, Phys. Rev. A **33**, 4033 (1986).
- [21] M. Hillery and L. Mlodinow, Phys. Rev. A **48**, 1548 (1993).
- [22] Abir Bandyopadhyay and Jagdish Rai, Phys. Rev. A **51**, 1597 (1995).

- [23] B. L. Schumaker, *Opt.Lett.***9**, 189 (1988); B. A. E. Saleh and M. C. Teich, *Phys.Rev.Lett.***58**, 2656 (1987).
- [24] R. P. Feynman, F. L. Vernon, Jr., and R. W. Hellwarth, *J. Appl. Phys.* **28**, 49 (1957).
- [25] J.M.Radcliffe, *J.Phys. A* **4**, 313 (1971).
- [26] F.T.Arecchi *et.al.* *Phy.Rev.A* **6**, 2211 (1972).
- [27] E.P.Wigner in *Group Theory and its applications to the Quantum Mechanics of Atomic Spectra*, Acad. Press, NY (1959); A.Vaglica and G.Vetri, *Opt. Comm.***51**, 239 (1984).
- [28] P. W. Atkins and J. C. Dobson, *Proc. Roy. Soc. Lond. A* **321**, 321 (1971).
- [29] M. Kitagawa and M. Ueda, *Phys. Rev. A* **47**, 5138 (1993).
- [30] S. M. Barnett and M. A. Dupertuis, *Journ. Opt. Soc. Am.***B 4**, 505 (1987).
- [31] K. Wodkiewicz and J. H. Eberly, *Journ. Opt. Soc. Am.* **B 2**, 458 (1985).
- [32] Arvind, B. Dutta, N. Mukunda and R. Simon, *Phys. Rev A* **52**, 1609 (1995); Arvind, Bdutta and N. Mukunda, private comm.
- [33] J. Schwinger in *Quantum theory of Angular Momentum*, ed. L. Beidenharn and H. van Dam, Academic Press, NY, 229 (1965).
- [34] L. Fonda, N. Mankoc-Borstnik and M. Rosina, *Phys. Rep.* **158**, 160 (1988).
- [35] J. Javanien and S. M. Yoo, *Phys. Rev. Lett.* **76**, 161(1996); *Phys. Rev. A* **53**, 4254 (1996).
- [36] S.Prasad, M.O.Scully, W.Martienssen, *Opt.Comm.*, **62**, 139 (1987).
- [37] R.A.Campos, B.E.A.Saleh, M.C.Teich, *Phy.Rev. A* **40**, 1371 (1989).
- [38] B.Huttner, Y.Ben-Aryeh, *Phy.Rev. A* **38**, 204 (1987).

- [39] J. Brendel, S. Schutrumpf, R. Lange, W. Martienssen and M. O. Scully, *Europhys. Lett.*, **5**, 223 (1988); C. K. Hong, Z. Y. Ou and L. Mandel, *Phys. Rev. Lett.*, **59**, 204 (1987).
- [40] U. Leonhardt, *Phys. Rev. A* **48**, 3265 (1993).
- [41] J.R.Pierce, *Journ. of Appl. Phy.* **25**, 179 (1954).
- [42] D. J. Love, G. H. C. New and M. A. Lauder, *Opt. Comn.* **59**, 177(1986).
- [43] W.K.Lai, V. Bužek and P.L.Knight, *Phys. rev. A* **43**, 6323 (1991).
- [44] B. W. Shore and P. L. Knight, *Journ. of Mod. Opt.* **40**, 1195 (1993) and references therein.
- [45] E. T. Jayens and F. W. Cummings, *Proc. IEEE* **51**, 89(1963).
- [46] R.A.Fisher, M.M.Nieto and V.D.Sandberg, *Phys.Rev. D***29**,6(1984)1107.
- [47] W. M. Zang, D. H. Feng and R. Gilmore, *Rev. Mod. Phy.* **62**, 867 (1990).
- [48] M.M.Nieto, *Phy.Rev. Lett.*,**18**,5(1967)182; P. Carruthers and M. Nieto, *Rev. Mod. Phy.* **40**, 411 (1968) and the references therein.
- [49] Susskind and Glogwer, *Physics* **1**, 49 (1964).
- [50] G. S. Agarwal, *Phys. Rev. A* **24**, 2889, (1981).
- [51] K. Blumm and H. Kleinpoppen, *Phy. Rep.* **52**, 203 (1979); K. Blumm, in *Prog. in At. Spect.*, Plenum, NY; J. N. Dodd and G. W. Series, *ibid.*; U. Fano, *Phys. Rev.* **90**, 577 (1953).
- [52] J. P. Dowling, G. S. Aagarwal, W. P. Schleich, *Phys. Rev. A* **49**, 4101 (1994).
- [53] A. Vaglica and G. Vetri, *Opt. comn.* **51**, 239 (1984).
- [54] D. F. Walls and P. Zoller, *Phys. Rev. Lett.* **47**, 709 (1981).

- [55] H. Goldstein in *Classical Mechanics*, Addison-Wesley, 425 (1980).
- [56] Y. Aharanov, D. Falkoff, E. Lerner and H. Pendleton, *Ann. Phys.* **39**, 498 (1966).
- [57] Ashcroft and Mermin, *Solid State Physics*, 2<sup>nd</sup> ed., Appendix-L.
- [58] R. W. Henry and S. C. Glotzer, *Am. J. Phys.* **56**, 318(1988).
- [59] M. Butler and P. D. Drummond, *Optica Acta*, **33**, 1(1986).
- [60] K.Svozil, *Phy.Rev.Lett.*,65(1990)3341.